

RPSEA

Technical Report

07123-03.02

***Near Miscible CO₂ Application to
Improve Oil Recovery for Small
Producers***

07123-03

October 22, 2010

Jyun-Syung Tsau
Associate Scientist
TORP, University of Kansas
The University of Kansas Center for Research, Inc.
2385 Irving Hill Road, Lawrence, KS 66045-7563

LEGAL NOTICE

This report was prepared by *University of Kansas Center for Research, Inc.* as an account of work sponsored by the Research Partnership to Secure Energy for America, RPSEA. Neither RPSEA members of RPSEA, the National Energy Technology Laboratory, the U.S. Department of Energy, nor any person acting on behalf of any of the entities:

- a. **MAKES ANY WARRANTY OR REPRESENTATION, EXPRESS OR IMPLIED WITH RESPECT TO ACCURACY, COMPLETENESS, OR USEFULNESS OF THE INFORMATION CONTAINED IN THIS DOCUMENT, OR THAT THE USE OF ANY INFORMATION, APPARATUS, METHOD, OR PROCESS DISCLOSED IN THIS DOCUMENT MAY NOT INFRINGE PRIVATELY OWNED RIGHTS, OR**

- b. **ASSUMES ANY LIABILITY WITH RESPECT TO THE USE OF, OR FOR ANY AND ALL DAMAGES RESULTING FROM THE USE OF, ANY INFORMATION, APPARATUS, METHOD, OR PROCESS DISCLOSED IN THIS DOCUMENT.**

THIS IS A TECHNICAL REPORT. THEREFORE, ANY DATA, CALCULATIONS, OR CONCLUSIONS REPORTED HEREIN SHOULD BE TREATED AS PRELIMINARY.

REFERENCE TO TRADE NAMES OR SPECIFIC COMMERCIAL PRODUCTS, COMMODITIES, OR SERVICES IN THIS REPORT DOES NOT REPRESENT OR CONSTITUTE AND ENDORSEMENT, RECOMMENDATION, OR FAVORING BY RPSEA OR ITS CONTRACTORS OF THE SPECIFIC COMMERCIAL PRODUCT, COMMODITY, OR SERVICE.

Abstract

This technical report discusses methodologies applied to 1) develop a geological model and a reservoir model, 2) conduct simulation study for history match of the primary production, and 3) investigate the effect of near miscible CO₂ injection on the oil recovery and CO₂ sequestration in a target oil field, Ogallah unit which is located at Trego County, Kansas.

The geological model developed is a primitive model based on well-log interpretation and cross-plotting method. An in-house developed correlation between porosity log and resistivity log was used to calculate porosity interpreted from microlog in most of the wells. The porosity, permeability, and initial water saturation were populated with geological software to construct the geological model. A commercial black oil simulator was used to history match the production history of the field. A compositional simulator was used to investigate the potential of CO₂ injection in improvement of oil recovery as well as sequestration at near miscible conditions.

A 47 acre lease containing four wells was extensively examined for the effect of CO₂ injection pressure, rate and pattern on the oil recovery efficiency. Due to the pressure support by the underling aquifer, the average reservoir pressure was always maintained at the near miscible condition during the CO₂ injection. Generally, the incremental oil recovery was increased with the injection pressure. The oil recovery efficiency was increased by 1.3 to 4.8% as a result of the injection of CO₂. The improved recovery efficiency results from the improvement of relative mobility ratio of the CO₂ and oil and the efficacy of CO₂ extraction. However, the recovery efficiency is significantly affected by the reservoir heterogeneity as shown in the pattern design where the recovery results depend on the placement of the injectors. The theoretical storage capacity of CO₂ in this 47 acre lease was estimated to be 1.58 BSCF. With 1.45 BSCF of CO₂ injected in 10 years, the effective storage capacity of CO₂ varied from 39 to 63%.

THIS PAGE INTENTIONALLY LEFT BLANK

TABLE OF CONTENTS

	<u>Page</u>
Table of Contents	i
List of Tables	ii
List of Figures	iii
1. Introduction	1
Background Information	2
2. Geological Model.....	3
Log Interpretation	4
Cross-plotting Method	6
Stratigraphy and Cross-section	10
3. Reservoir Model and Simulation	14
History Match of Primary Production.....	16
Simulation of Carbon Dioxide Injection.....	24
One CO ₂ Injector.....	25
Two CO ₂ Injectors.....	29
4. Summary	40
References	41

List of Tables

		<u>Page</u>
Table 1	Type of well logs available at Ogallah unit	4
Table 2	Visual indication of rock type: shale, dolomite, sandstone, and granite-wash	5
Table 3	Ogallah wells with lithology information available	5
Table 4	PVT data used in simulator	17
Table 5	Well block properties at well locations	24
Table 6	Comparison of incremental oil and water production in 10 years of CO ₂ injection (CO ₂ injected at well 3-3)	26
Table 7	Comparison of incremental oil and water production in 10 years of CO ₂ injection (CO ₂ injected at well 3-2)	26
Table 8	Result of case study with CO ₂ injection at BHP of 1300 psi	36
Table 9	Result of case study with CO ₂ injection at BHP of 1200 psi	37
Table 10	Result of case study CO ₂ injection at 200 MSCF/day/well	38

List of Figures

		<u>Page</u>
Figure 1	Ogallah unit, Trego County, Kansas	2
Figure 2	Porosity overlays of Well 4-16.....	3
Figure 3	Microlog (ϕ_{ML}) porosity cross plotted with (a) Neutron Porosity	4
Figure 4	Derived average porosity (a) and water saturation (b) plotted with depth for well 14-1.....	9
Figure 5	Contour grid of the Ogallah formation tops and the cross-section profiles.....	9
Figure 6	Cross section of wells indicated as Line A-A'	10
Figure 7	Isopach of the net-pay in Ogallah based on log interpretation	13
Figure 8	Porosity-permeability correlation of Arbuckle Group	13
Figure 9	Structure top map of Ogallah Unit	14
Figure 10	Example of cross section view of Ogallah Unit.....	15
Figure 11	Permeability and porosity of Arbuckle dolomite and Reagan sandstone.....	15
Figure 12	Annual production history of Lease 3, E. A. Scott.....	16
Figure 13	Relative permeability curves for oil and water	18
Figure 14	History match of oil production in well 3-2	19
Figure 15	History match of water production in well 3-2	19
Figure 16	History match of oil production in well 3-3	20
Figure 17	History match of water production in well 3-3	20
Figure 18	History match of oil production in well 4-12	21
Figure 19	History match of water production in well 4-12.....	21
Figure 20	History match of oil production in well 4-13	22
Figure 21	History match of water production in well 4-13	22
Figure 22	Average reservoir pressures of Ogallah unit and Lease E. A. Scott	23
Figure 23	Grid system of Lease 3, E. A. Scott.....	25
Figure 24	Incremental oil productions at well 3-2 when CO ₂ was injected at well 3-3 ...	27
Figure 25	Reduction of water production at well 3-2 when CO ₂ was injected at well 3-3	27
Figure 26	Incremental oil productions at well 3-3 when CO ₂ was injected at well 3-2 ...	28

	<u>Page</u>
Figure 27	Reduction of water production at well 3-2 when CO ₂ was injected at well 3-3 28
Figure 28	Pattern design of lease 3 for CO ₂ injection 29
Figure 29	CO ₂ distributions after 10 years of injection, Case A1 30
Figure 30	CO ₂ distributions after 10 years of injection, Case B1 31
Figure 31	CO ₂ distributions after 10 years of injection, Case C1 31
Figure 32	CO ₂ distributions after 10 years of injection, Case D1 32
Figure 33	CO ₂ distributions after 10 years of injection, Case E1 32
Figure 34	CO ₂ distributions after 10 years of injection, Case F1 33
Figure 35	Comparison of oil recovery factors at Lease 3 33
Figure 36	Average reservoir pressures at Lease 3 with/without CO ₂ injection..... 34
Figure 37	Lease 3 production performance without CO ₂ injection 39

1. Introduction

This project describes a research program to evaluate the application of CO₂ displacement at near miscible pressures for improved oil recovery (IOR) and carbon sequestration for small producers. Two technical reports are prepared at the completion of this project. The first technical report discusses fundamental studies of phase behavior for the CO₂/crude oil system and the displacement process at pressures near miscible condition which is commonly referred to at pressure below but near minimum miscible pressure (MMP). The second technical report describes the construction of a geological model, a reservoir model with a commercial simulator, and discusses the simulation results on improvement of oil recovery by CO₂ injection and the potential for carbon sequestration in oil reservoirs at near miscible conditions.

This report is the second technical report of the project. It summarizes the methodologies applied to 1) develop a geological model and a reservoir model, 2) conduct simulation study for history match of the primary production, and 3) investigate the effect of near miscible CO₂ injection on the oil recovery and CO₂ sequestration in the target oil reservoir. The target oil field, Ogallah unit is located at Trego County, Kansas. The unit is currently operated by Carmen Schmitt, Inc. The unit produces from Arbuckle formation (3950-4060 ft) and other formations above the Arbuckle (Marmaton and Lansing-Kansas City).

The geological model developed in this study is a primitive model based on well-log interpretation and cross-plotting method. Due to the lack of advanced log data in the early 1950 when the Ogallah unit was developed, the reservoir porosity was calculated by resistivity log interpretation and calibrated with a correlation developed from a modern suite of logs of an infill drilled well in 2000. The permeability estimation was based on a correlation published by Byrnes *et al.* (1999) in which the permeability and porosity relationship is developed from core plug measurement representing the Arbuckle group petro facies. The initial water saturation was calculated using Archie equation along with the data derived from the resistivity logs. All the data derived from geological study were populated with PETRA software (IHS Inc.) to create a geological model. The phase behavior model developed from the phase behavior study as reported in the first technical report (Tsau *et al.*, 2010) was used with the geological model to form the reservoir model. A commercial simulator, IMEX (Computer Modeling Group, Inc.) was used to simulate the primary production history. A compositional simulator, GEM (CMG

Inc.) was used to investigate the potential of using carbon dioxide at near miscible condition for improvement of oil recovery as well as CO₂ sequestration.

Background Information

Arbuckle reservoirs are a significant resource in Kansas for improved oil recovery. These reservoirs have produced an estimated 2.2 billion barrels of oil representing 35% of the 6.1 billion barrels of oil of total Kansas oil production (Franseen *et al.*, 2004). Most Arbuckle reservoirs have active water drives which have maintained reservoir pressure at 1000-1100 psig for nearly 50 years even though millions of barrels of fluid have been produced. Initial studies of CO₂ miscible flooding indicated that miscibility is not achievable at the reservoir operating pressure in most Arbuckle reservoirs. For example, the Arbuckle reservoir oil in the Bemis-Shutts field has a MMP of 1400 psi while the current operating pressure is 1100 psi in a large portion of the field (Franseen *et al.*, 2003). The Arbuckle reservoir in this study, Ogallah unit has a MMP of 1350 psi while the current reservoir operating pressure is in the neighborhood of 1150 psig. The core flow test in the laboratory study indicated that at least 50% of remaining oil can be recovered by CO₂ injection at current reservoir operating pressure (Bui *et al.*, 2010).

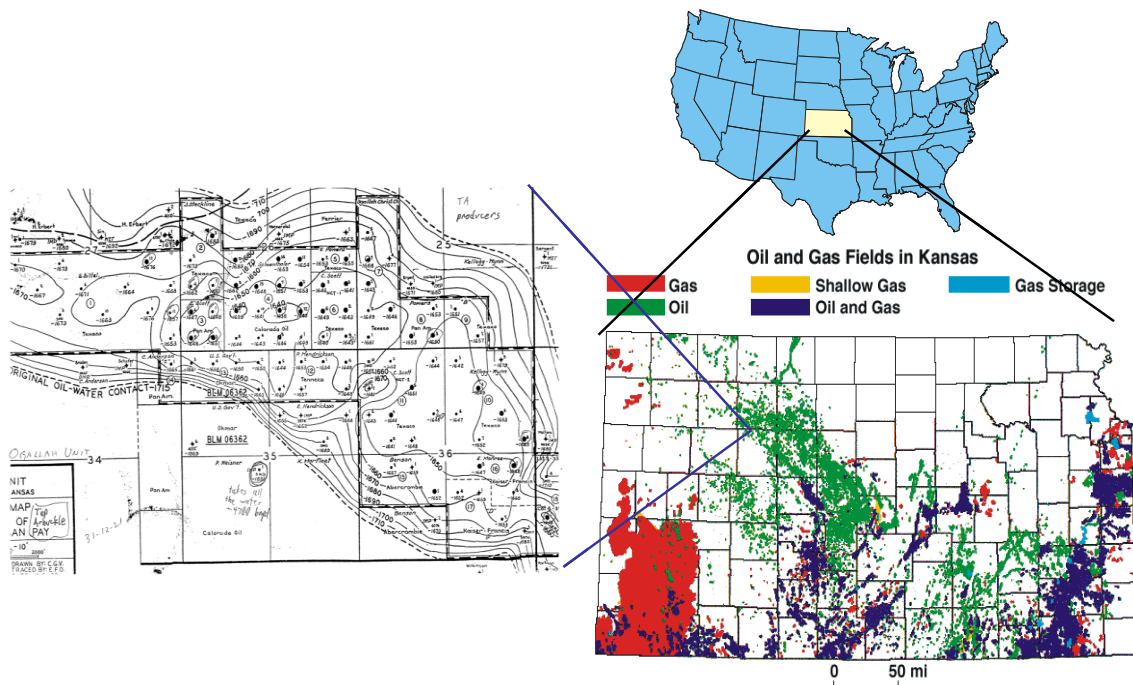


Figure 1 Ogallah unit, Trego County, Kansas

The Ogallah field is located at Trego County, Northeastern Kansas along the east side of the Nemaha uplift. The primary producing formation in this study is the Arbuckle at 3950-4060 ft. The formation is associated with structural high at central Kansas uplift and is thin to absent in parts of Northeastern Kansas (Franseen, *et al.*, 2004).

The field database contained pre-60's gamma ray, resistivity and microlog from most wells. Only one infill drilled well was logged with modern gamma-ray, resistivity and neutron-density log in year 2000. To prepare the log measurements for analysis, the logs were digitized on foot-by-foot basis. The relatively short penetration of logged-depth, at approximately 10 feet, into the Arbuckle signifies the early field development of Ogallah. Franseen *et al.* (2004) in "*The Geology of Kansas, Arbuckle Group*" explained that the completion practice is shaped by the high unconformity structure of Arbuckle and a semi-infinite aquifer underlying the reservoir rock. The completion practice therefore has resultant limited description of the lower zone.

Fourteen cored well data were available across the Ogallah field when the wells were drilled in the early 1950. From the lithology description presented in the core analysis report, the upper carbonate sequence (Arbuckle) was found to form a few streaks of dolomite-sand with variable thickness of crystalline-dolomite. The dolomite was characterized by permeability in the range of 0.01 to 150 md and low porosity from 1 to 12%. The lower Precambrian sequence of the reservoir was deposited with Reagan sandstone showing good permeability ranging from 0.01 to 400 md and higher porosity varied from 1 to 20%.

Primary production of the Ogallah started in 1951. Well production history shows that no water was produced before 1960. Water breakthrough in producers started after 1960. Due to the high water production, wells were work over with well deepening, formation plug-back and perforation at upper interval. At the peak of production in 1969, the Ogallah field had 85 producing wells. The field was producing 1.07 MMBO/year with cumulative production of 11.37 MMBO by 1969. After 1969, the field commenced commingle-production from Lasing Kansas City formation (LKC) and half amount of those wells were shut in at 1989 due to economic decline. The Ogallah field was unitized in 1991 and the number of active producers since then was reduced to 18.

2. Geological Model

The geological model developed is a primitive model based on well-log interpretation and cross-plotting method. The reservoir porosity was calculated by using resistivity log which is later calibrated with a correlation developed by using a modern suite of logs from an infill drilled well in 2000. The permeability estimation was based on a correlation published by Byrnes *et al.* (1999). The initial water saturation was calculated using Archie equation along with data derived from the calibrated resistivity logs. Detailed discussions on construction of this primitive model are described in the following sections:

Log Interpretation

Prior to estimating the reservoir properties quantitatively, a preliminary analysis was conducted to identify the Arbuckle formation by reviewing the well logs, formation information described by the geologists and log measurements. The logs available for analysis include gamma-ray, resistivity (laterolog, microlog, microlaterolog and guard), and neutron-gamma logs. Table 1 lists the number of different type of logs available for this study. From the visual-investigation of formation signature among the logs, it reveals that the formation lithology depends on the relative value from the comparisons of two or more log trend. Table 2 describes the guideline used to identify the formation by this visual investigation method. Four groups of rock type were classified based on the logging measurements.

The initial reservoir description and interpretation of the well logs were developed based on the lithology description from each well. Mapping of the Ogallah unit stratigraphy surface, the sequence of the deposition and correlation of formation tops relied on lithology information which is not available from most of the wells. The number of wells with lithology information available is summarized in Table 3 in which 11 wells contain identifiable data of top of Graitewash while 17 wells have information available for Reagan formation top and 28 wells have data available for Arbuckle formation top.

Table 1 Type of well logs available at Ogallah unit

Well Log Description	No. of Wells
Neutron-gamma	13
Microlog, microresistivity	15
Resistivity	28
Gamma-ray	28

Table 2 Visual indication of rock type: shale, dolomite, sandstone, and granite-wash

Rock-Type	Gamma-ray	Neutron-gamma	Resistivity logs (resistivity, guard, laterolog, microlog, microlaterolog)
Shale	High	High	Low
Dolomite	Low	Low	High, oil-bearing zone.
Sandstone	Low	Low	Low, assuming that sandstone containing highly conductive pore fluid.
Granite-wash	High	Low	High

Table 3 Ogallah wells with lithology information available

Formation Identified	No. of Wells
Arbuckle	28
Reagan	17
Granite-wash	11

Neutron-gamma (GRN) Log Analysis

Neutron-gamma log were recorded in counts per second (CPS) or API unit. A logarithmic scale was derived using the high-low porosity method. The high porosity value (ϕ_h) was in the range of 0.20-0.30 and the low porosity (ϕ_l) was in the range of 0.01-0.05. The equation for porosity computation is shown as follows,

$$m = \frac{\log(\phi_h/\phi_l)}{(CPS_h - CPS_l)} \quad (1)$$

$$c = \frac{\phi_h}{10^{(CPS_h \times m)}} \quad (2)$$

$$\phi_n = c \times 10^{(NCPS \times m)} \quad (3)$$

where CPS_h is GRN counts at high porosity point, CPS_l is the GRN counts at low porosity point, and $NCPS$ is the neutron log readings.

Microlog and Microlaterolog Analysis

The microlog and microlaterolog porosity (ϕ_{ml}) was derived from the rearrangement of classical Archie equation. No shale correction was applied to the equation. To calculate the porosity, the mud filtrate resistivity (R_{mf}) at formation of interested was used, which is derived from the value obtained from log header and calibrated to formation temperature. The expression of microlog and microresistivity porosity is estimated as,

$$\phi_{x0} = \left[\frac{A}{(R_{x0}/R_{mf}) \times S_{x0}^n} \right]^{1/m} \quad (4)$$

where S_{x0} is assumed to be 1.0 for low porosity zone and 0.70 for the hydrocarbon bearing zone.

Water Saturation

The water saturation was estimated from Archie equation (5). To compute the water saturation, R_t was read from the resistivity logs (laterolog and guard log), R_w was estimated at the temperature of interested formation depth, and effective porosities was calculated from porosity log and microlog.

$$S_w = \left[\left(\frac{A}{\phi^m} \right) \times \left(\frac{R_w}{R_t} \right) \right]^{1/n} \quad (5)$$

In this study, R_w , 0.130 was estimated at formation temperature, 110 °F. Parameters of carbonate values, $m = 2$, $n = 2$, and $a = 1$ were applied to compute the water saturation profile for each well.

Cross-plotting Method

Porosity is normally derived from single porosity method for wells with good porosity logs such as neutron density and sonic log. However, very limited porosity data are available at time of the development of the Ogallah unit in the early 1950. Most logs in Ogallah unit are either micrologs or microlaterlogs which are used as porosity indicators. The porosity derived from these logs is generally affected by the R_{x0} measured at the formation surrounding the tool. In year 2000, a modern suit of logs was conducted in an infill drilled well, 4-16 at Schoenthaler lease. It provided the opportunity to correlate the porosity derived from neutron density, sonic porosity log with resistivity logs in this well. With the new correlation developed from well 4-16, the porosity estimation from all the old resistivity logs becomes feasible.

Well 4-16 was drilled with a total depth of 4100 ft. It was logged with modern gamma-ray, neutron, density, spontaneous potential, resistivity log and microlog. From the geological report, Arbuckle formation was located approximately at 3990 – 4050 ft. Fair oil staining was observed for the first eight feet sandy-dolomite in the interval.

Porosity derived from neutron and density log was cross-plotted with porosity determined from microlog in well 4-16 to develop a reasonable correlation between porosity log and

microlog. This cross-plotted relationship was used to derive the porosity from microlog in wells where no porosity log is available.

Well 4-16 Cross-plot Porosity

Graphical comparison of well 4-16 porosity logs using porosity overlay is illustrated in Figure 2. Both neutron porosity and density porosity are recorded in limestone porosity unit. The separation of the porosity curves is an indicative of a certain type of lithology. At the interval of 3972-4003ft, the separation of curves where ϕ_N (PHIN) > ϕ_D (PHID) is corresponding to shale. A sandstone interval with $\phi_N < \phi_D$ is found at 4004-4019 ft and 4033-4051 ft. Lack of curve separation at interval of 4033-4051 ft, is an indication of dolomite streak.

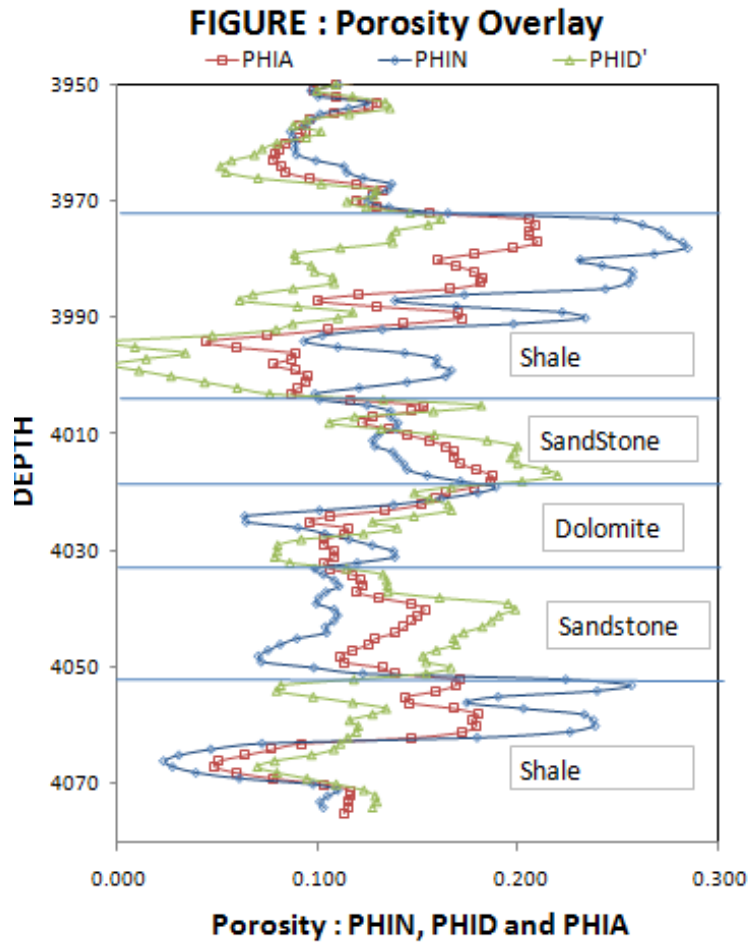


Figure 2 Porosity overlays of Well 4-16

In Figure 2, dolomite and sandstone layers indicate an average porosity (PHIA) of 0.12 and 0.14, respectively. The calculated average porosity data from this well is then cross-plotted

with microlog porosity at each corresponding depth interval to derive the correlation between the averaged porosity log and microlog. Figure 3 shows the relationship between the porosity response of microresistivity logs (ϕ_{ML}) with the neutron porosity (ϕ_N), density porosity (ϕ_D) and average porosity (ϕ_{AV}). The cross-plot demonstrates a conversion relationship of the porosities corresponding to reservoir rock lithology. The developed correlation is used to convert porosities derived from resistivity logs to representative porosities in other wells.

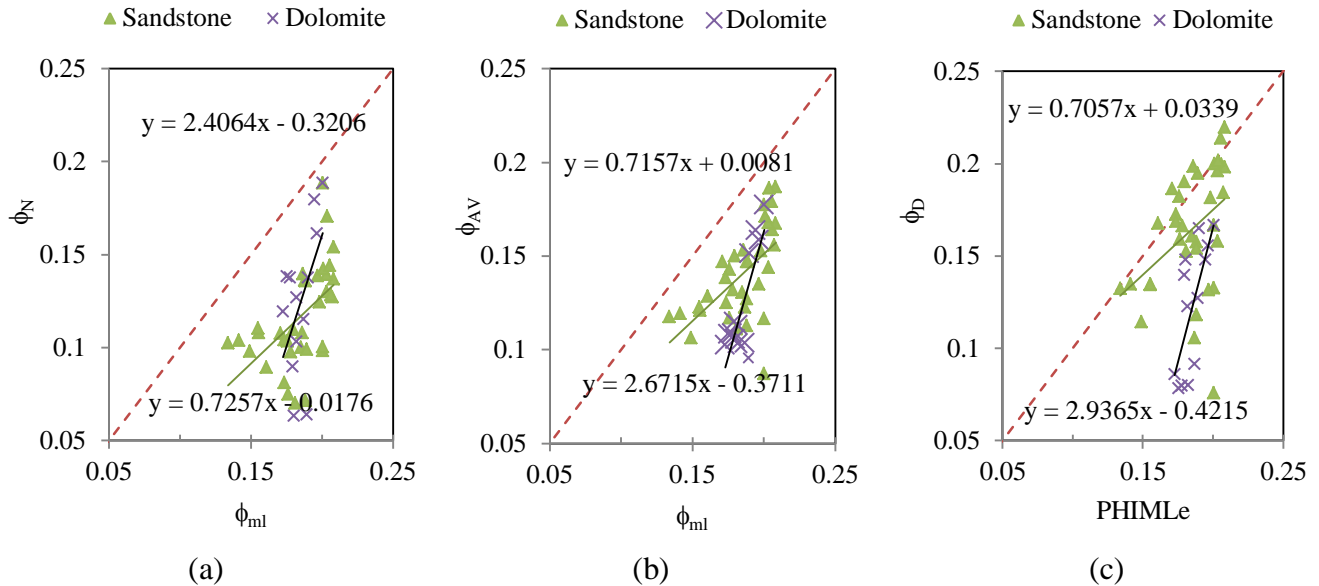


Figure 3 Microlog (ϕ_{ML}) porosity cross plotted with (a) Neutron Porosity (ϕ_N) (b) Average Porosity (ϕ_{AV}) (c) Density Porosity (ϕ_D) for the Arbuckle of well 4-16. The shale effect was included.

Example of well 14-1 Porosity Calculation

Well 14-1 is a producing well logged with gamma-ray, resistivity and microlog. It was drilled in year 1952 with Arbuckle top identified at 3989 ft. Example of converting microlog data to an averaged porosities by means of the cross plotting method is described with a set of microlog data as follows.

1. The lithology of well 14-1 was first defined based on geology description from geological report and the visual interpretation method given in Table 2.
2. The microlog porosity was computed using microlog of well 14-1.
3. The microlog porosity was converted to neutron porosity, average porosity and density porosity using the derived relationship from well 4-16.
4. The water saturation was calculated with the average porosity derived in step 3.

Figure 4 (a) shows the final converted porosity and Figure 4 (b) shows the derived water saturation profile as calculated by equation (5).

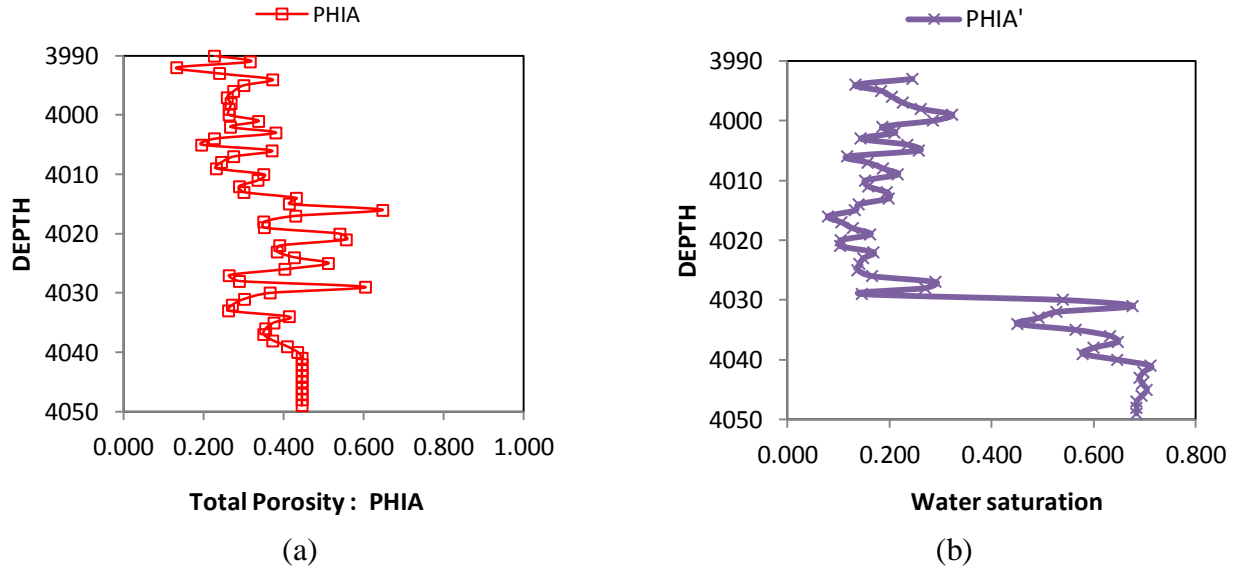


Figure 4 Derived average porosity (a) and water saturation (b) plotted with depth for well 14-1.

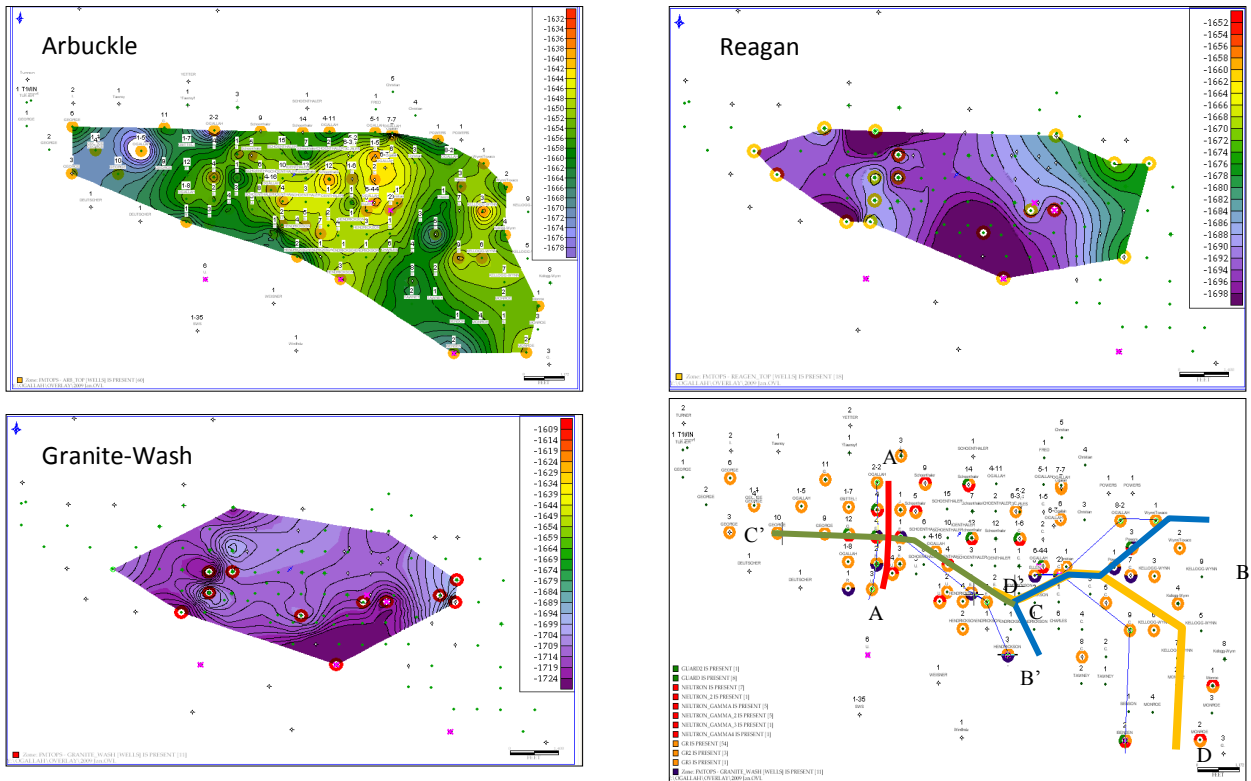


Fig. 5 Contour grid of the Ogallala formation tops and the cross-section profiles

Stratigraphy and Cross-section Profiles

The stratigraphy and lithology profile of wells were constructed based on the formation top markers. The Ogallala net-pay mapped based on the sequence of deposition is shown in Figure 5.

The cross sections of Ogallala are presented in Figure 6. From the cross section, it is seen that Arbuckle formation is generally located at high structure underlain by Reagan sandstone and Granite-wash. Reagan formation is absent in some area in the lease where Arbuckle formation is found at low structure. The isopach maps of the net-pay for Arbuckle and Reagan formations are shown in Figure 7.

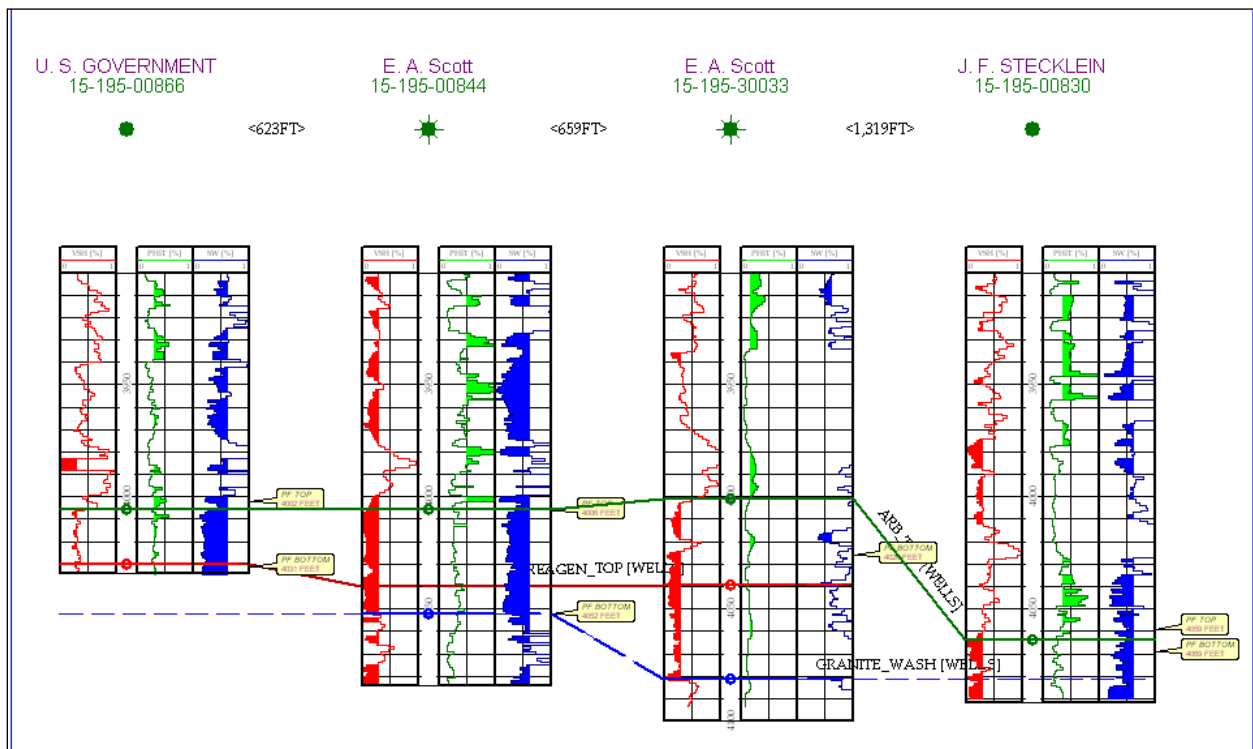


Figure 6a Cross section of wells indicated as Line A-A' (red line in Figure 5)

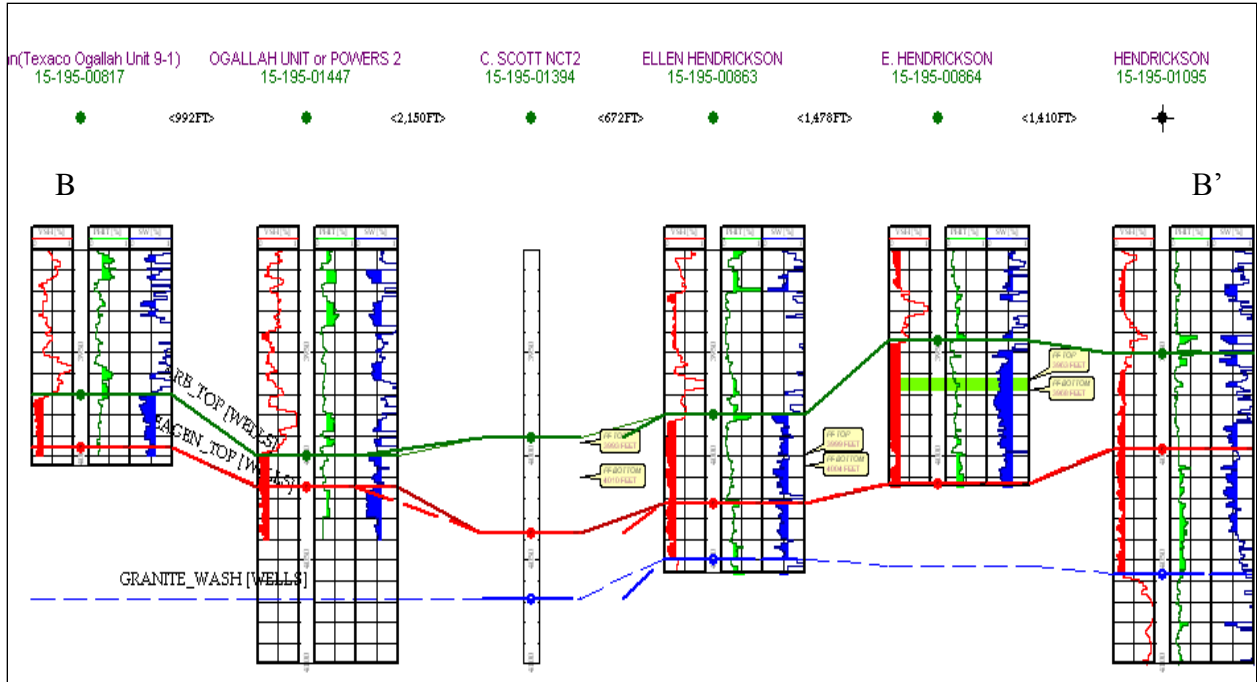


Figure 6b Cross section of wells indicated as Line B-B' (blue line in Figure 5)
Well UWI: 15-195-01394 has incomplete laterolog and microlog.

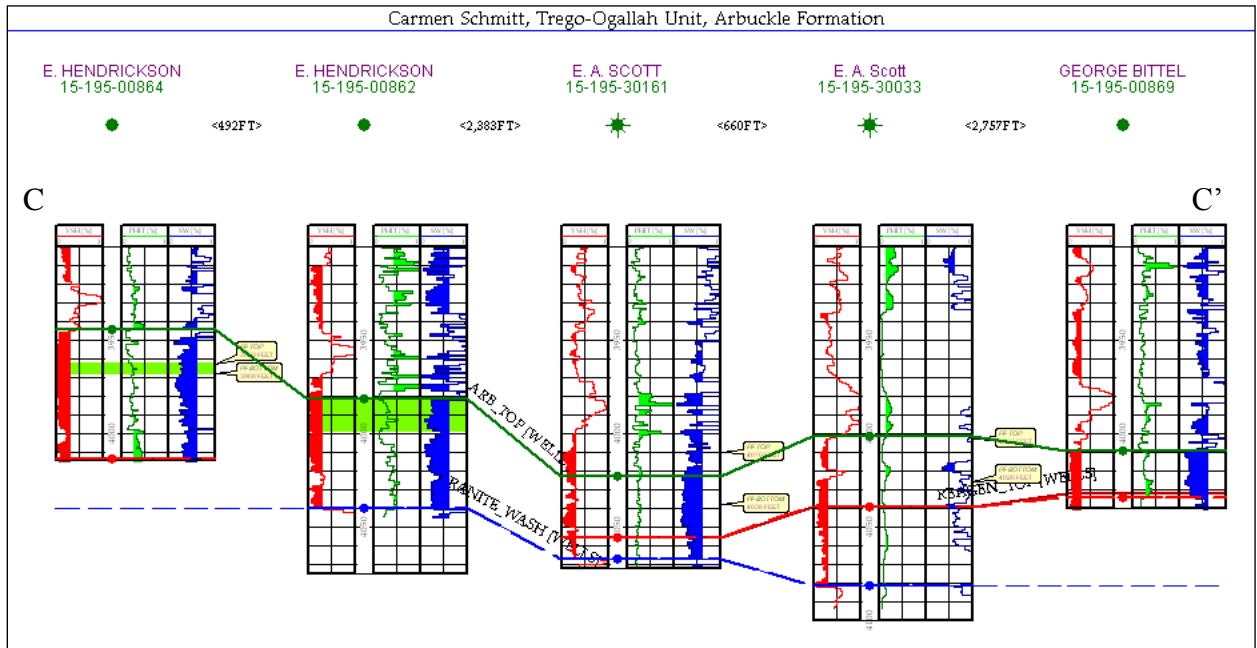
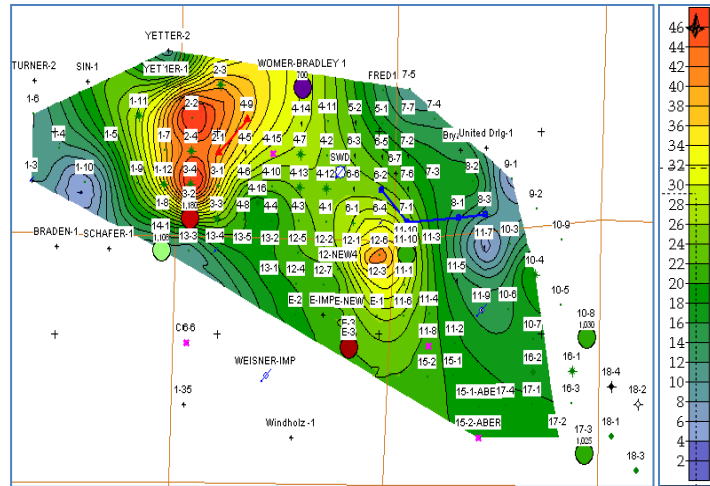


Figure 6c Cross section of wells indicated as Line C-C' (green line in Figure 5)



(b) Reagan sandstone

Figure 7 Isopach of the net-pay in Ogallah based on log interpretation

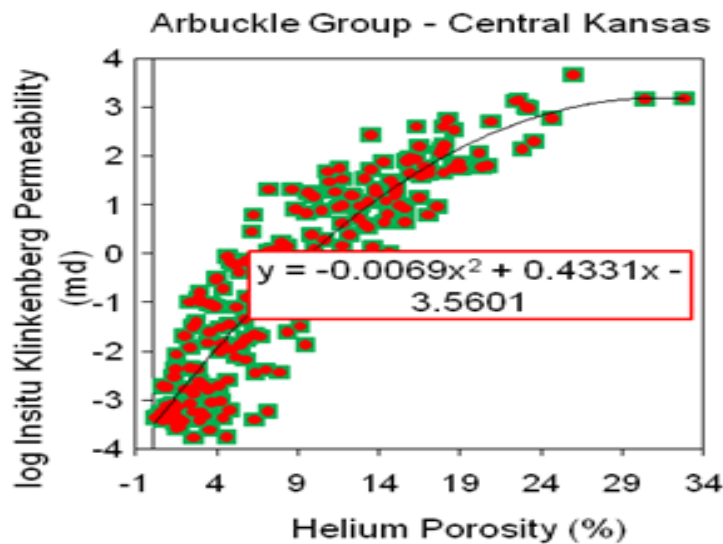


Fig. 8 Porosity-permeability correlation of Arbuckle Group (Byrnes *et al.*, 1999)

Porosity-Permeability Distribution

The permeability calculation was based on the permeability correlation of Arbuckle Group, Central Kansas which was published by Byrnes *et al.* (1999). In that study, Byrnes *et al.* collected petrophysical data from a number of core-plug samples of different Arbuckle facies and related the facies and matrix properties to reservoir character. The equation shown in Figure 8 represents the typical correlation of petrophysical property in Arbuckle formation. The

correlation was adopted to calculate the permeability as a function of porosity for Arbuckle formation in Ogallah unit.

Geological software, PETRA was used to construct the geological model with all the reservoir properties collected through the aforementioned methods. The spatial distribution of the Ogallah reservoir properties such as porosity, permeability, water saturation and net-pay gridded surfaces were subsequently exported to Builder, a pre-processing application of commercial simulator, IMEX for further construction of a reservoir model.

3. Reservoir Model and Simulation

Black oil simulator, IMEX was used to perform history match of primary production in Ogallah unit. The geological model was exported to Builder to construct a reservoir model along with PVT data, relative permeability data and recurrent data of well location, perforation depth and production history. The model was discretized with 127 blocks in east-west direction, 70 blocks in north-south direction and 8 layers in vertical direction. The grid block size was 110 feet in length and 110 feet in width. The thickness of each grid varied. Figure 9 presents the structure top of the oil field and the location of 103 wells. Figure 10 shows an example of the cross-section view of the layers consisting of Arbuckle dolomite and Reagan sandstone. The Granite wash was not included in the model as it is assumed to be part of the aquifer underling the reservoir. The aquifer was modeled with Carter-Tracery method to simulate the aquifer as a bottom water drive aquifer.

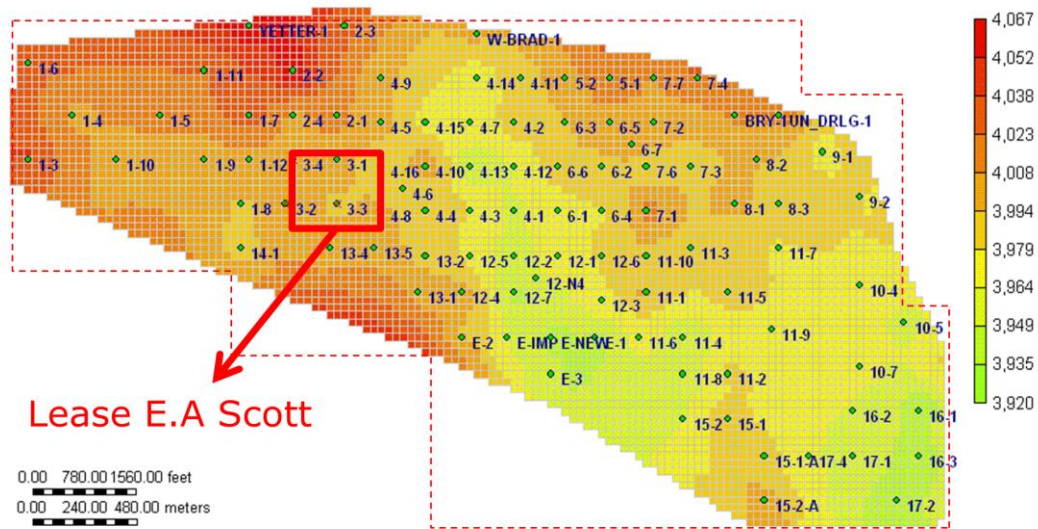


Figure 9 Structure top map of Ogallah Unit

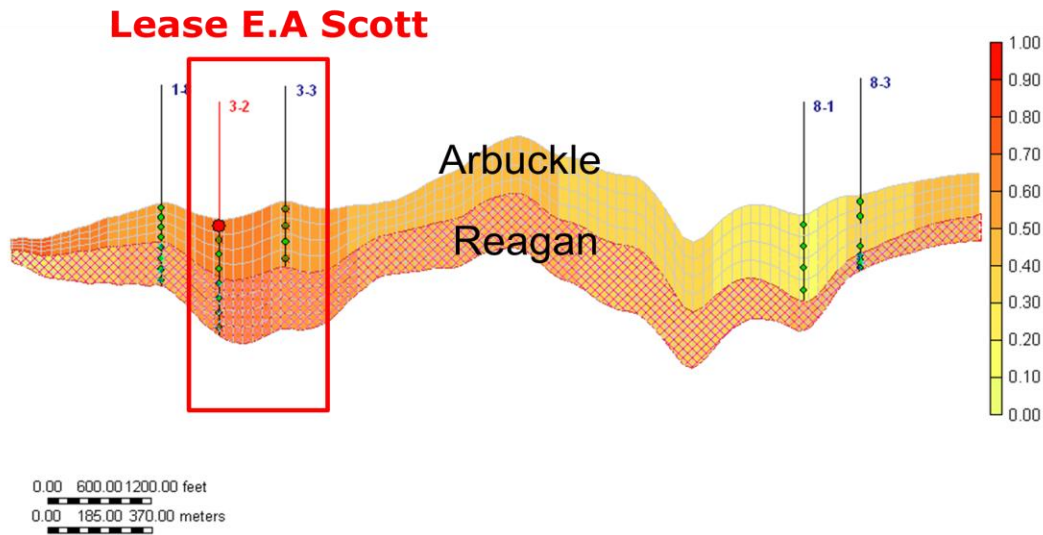


Figure 10 Example of cross section view of Ogallah Unit

Figure 11 presents the permeability and porosity distribution in the Arbuckle and Reagan layer of the model. High permeability and porosity are generally observed in the central-southwest part of the field which includes part of Lease 1, (G. Bittle), Lease 3, (E.A. Scott), and Lease 13, (U.S. Government).

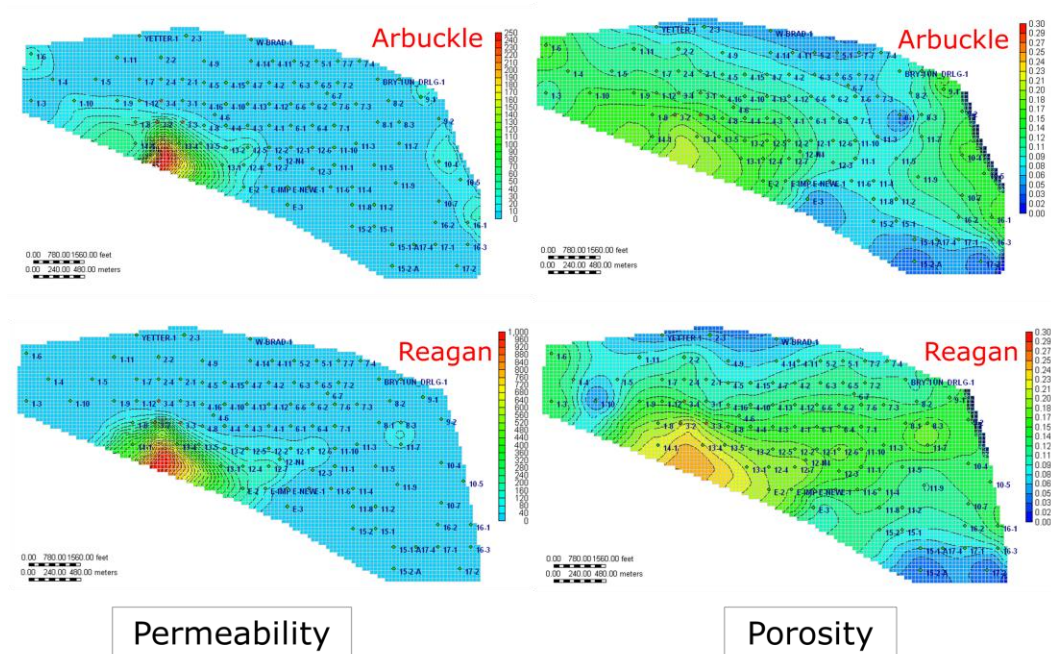


Figure 11 Permeability and porosity of Arbuckle dolomite and Reagan sandstone

History Match of Primary Production

Primary production of the Ogallah started in 1951. Well production history shows that no water was produced before 1960. Water breakthrough in producers started after 1960. At the peak of production in 1969, the Ogallah field had 85 producing wells. The field was producing 1.07 MMBO/year with cumulative production of 11.37 MMBO by 1969. After 1969, the field commenced commingle-production from LKC formation and approximately half number of these wells were shut in at 1989 due to economic decline. The Ogallah field was unitized in 1991 and the number of active producers since then was reduced to 18.

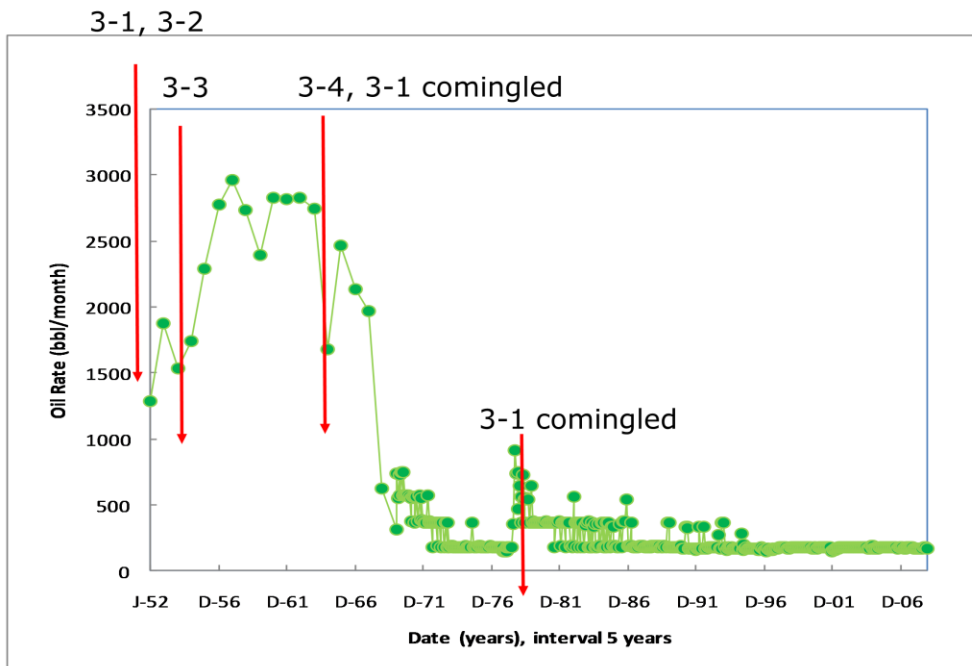


Figure 12 Annual production history of Lease 3, E. A. Scott

Individual well production history in Ogallah unit was not recorded in the early years of production. Most recent record for individual active producer was from 1991 onwards. Nevertheless, Kansas Geological Survey database has production record of each lease in the unit. Figure 12 shows the annual production history of Lease 3, E. A. Scott. Production in Lease 3 started in 1952 when well 3-1 and 3-2 were first drilled and produced from Arbuckle formation. Well 3-3 started production from Arbuckle in 1955. The total production rate from all three wells stabilized at around 2700 BO/month. The production rate started to decline from 1963. In 1965, well 3-4 was drilled and produced from Arbuckle and Lasing-Kansas City (LKC). At the

late of 1965, LKC-F was perforated in well 3-1 to have a comingle production with Arbuckle. The production rate started decline significantly after water breakthrough. Another apparent rate increase occurred in 1977 when well 3-1 was perforated at upper formations, LKC-A and Topeka.

It is challenging to history match the primary production performance of the whole unit as there is insufficient field data for each individual producer, and in most cases, the production is commingled with other formations on top of Arbuckle group. Because of the limitation of data, the effort to history match was directed toward wells with detailed production record from Arbuckle group only. Two wells, well 3-2 and 3-3 in Lease 3 (E.A Scott), and two wells, 4-12 and 4-13 in Lease 4 (Schoenthaler), are produced from Arbuckle formation. The history match on these four wells is discussed in the following sections.

The production of the Ogallah unit is primarily attributed to natural water drive as the reservoir pressure has been maintained at above 1150 psi for more than 50 years. To simulate the primary production by the bottom water drive, black oil simulator, IMEX is used to history match the production performance. The volumetric performance of reservoir fluids at various pressure levels are tabulated in Table 4. These data are derived from the laboratory studies of PVT of reservoir fluid in a companion technical report (Tsau, *et al.* 2010)

Table 4 PVT data used in simulator

P (psia)	Rs (scf/stb)	Bo (rb/stb)	z	viso (cp)	visg (cp)
15	3.5	1.021	0.999	4.124	0.0124
412	62.8	1.039	0.964	2.906	0.0127
809	136.7	1.063	0.933	2.176	0.0133
1206	218.6	1.091	0.908	1.735	0.0140
1603	306.1	1.122	0.889	1.445	0.0148
2000	398.1	1.157	0.878	1.241	0.0157

Relative permeability curves for two flow units (Arbuckle and Reagan) were modeled using modified Corey-type equations (Corey, 1954) where S_{wc} was obtained from the laboratory measurement. The modified Corey relative permeability equations used were:

$$k_{ro} = k_{roS_{wi}} (1 - S_{WD})^m \quad (6)$$

$$k_{rw} = k_{rwS_{ORW}} (S_{WD})^n \quad (7)$$

$$S_{WD} = (S_w - S_{WC}) / (1 - S_{ORW} - S_{WC}) \quad (8)$$

where m is the exponent of the oil relative permeability and n is the exponent of water relative permeability. Figure 13 shows the oil-water relative permeability curves used in the simulation. The m - and n -exponent used are 5 and 2 respectively. The end-points residual oil and water saturation are both 0.25. For Arbuckle formation parameters used were: $k_{ro_{S_{wi}}} = 1.0$, $k_{rw_{SORW}} = 0.18$; for Reagan formation parameters used were: $k_{ro_{S_{wi}}} = 1.0$, $k_{rw_{SORW}} = 0.07$.

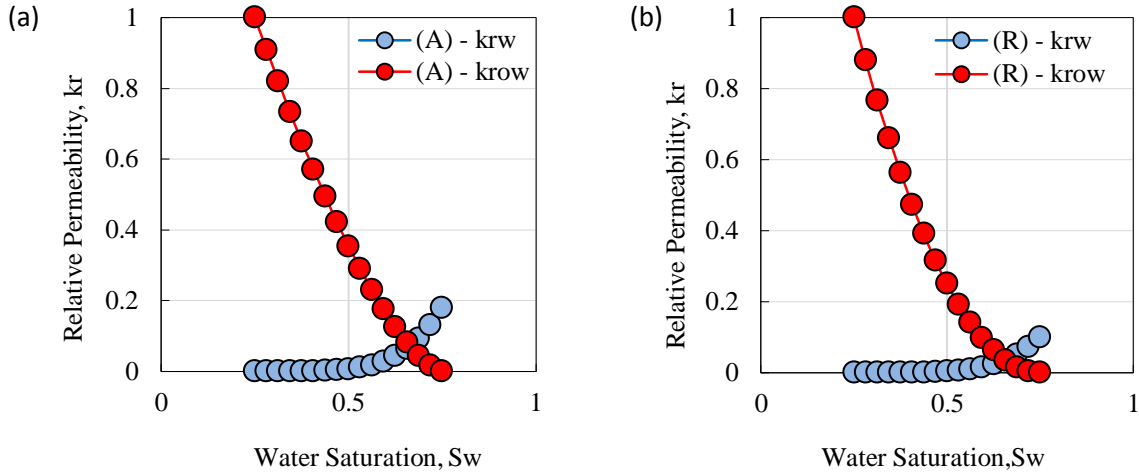


Figure 13 Relative permeability curves for oil and water. (a) Arbuckle formation, (b) Reagan formation.

The initial reservoir pressure was assumed to be 1200 psia based on DSTs conducted in the early year of production. The rate constraint was applied to the wells when prorate production was imposed. Otherwise, the pressure constraint was applied to the producers at a given bottomhole pressure when the record was available or pumped off when it was not available. During the process of history match, properties being adjusted include horizontal permeability, end point of relative permeability and initial water saturation.

Some of the production history match results are presented in Figure 14 to Figure 21 where the symbols represent the field data while the curves represent the simulation results. In most of these plots, the production rate of each individual well is not available prior to 1991. At the early time of simulation, the oil production was controlled at a given rate in the model to represent the prorate production stipulated by the government at the early stage of the development. In general, the production history is reasonably well matched.

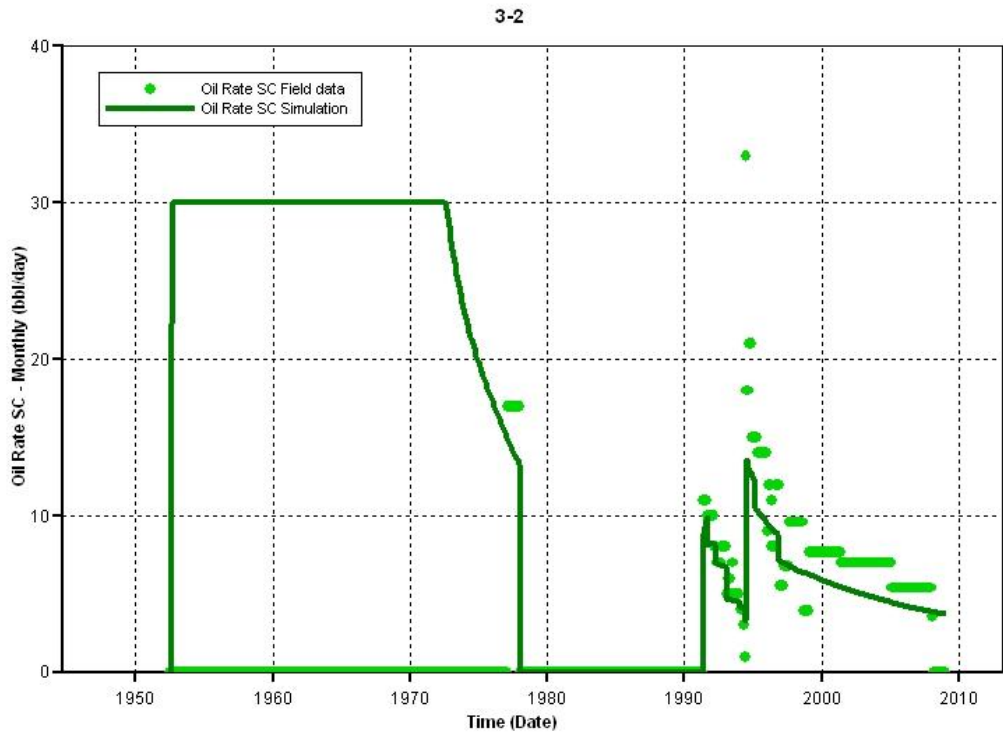


Fig. 14 History match of oil production in well 3-2

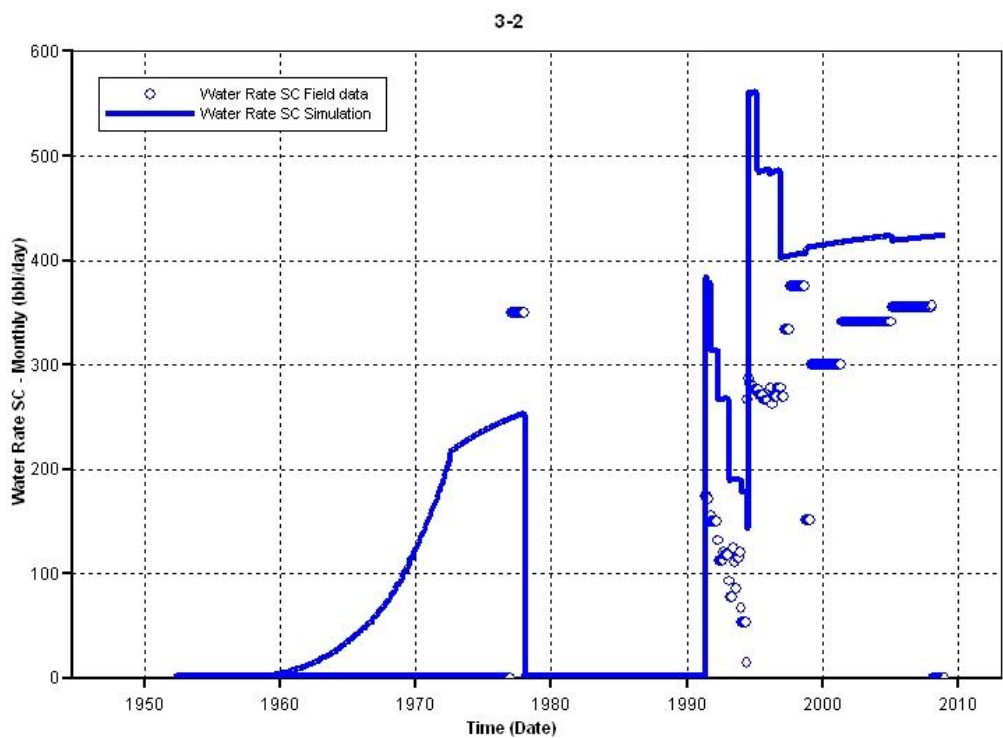


Figure 15 History match of water production in well 3-2

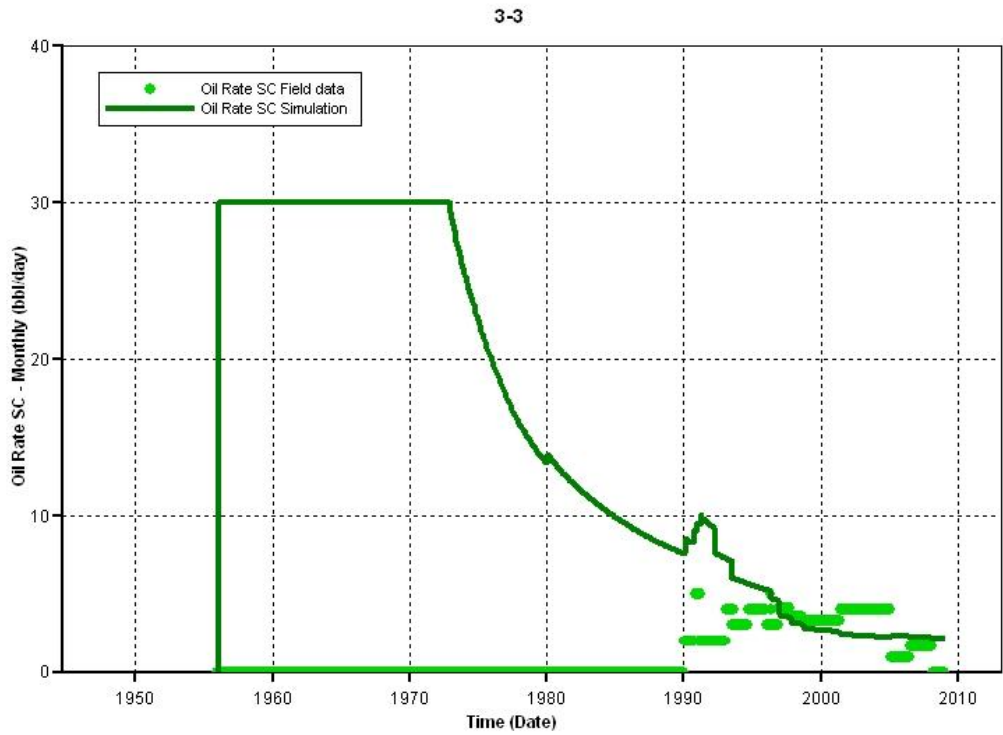


Fig. 16 History match of oil production in well 3-3

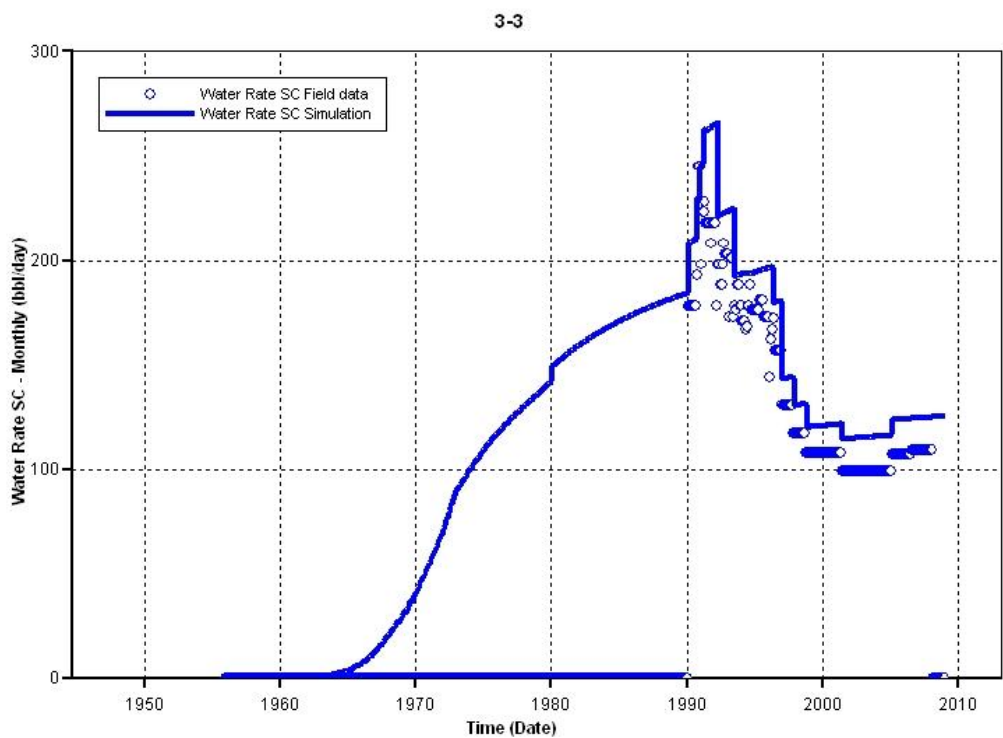


Figure 17 History match of water production in well 3-3

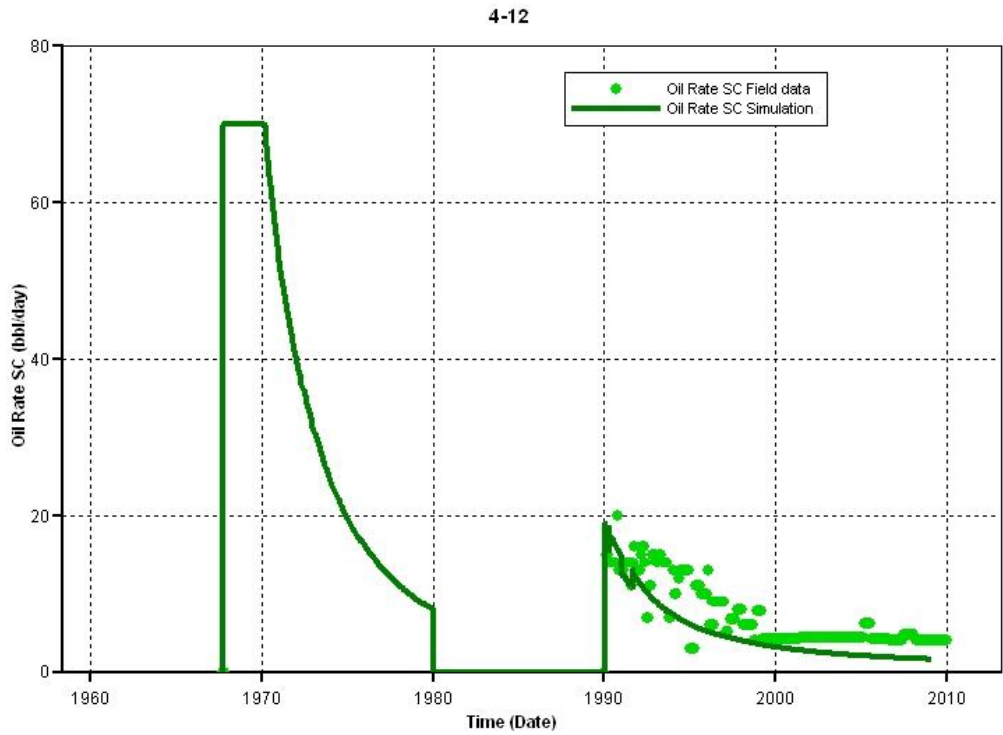


Fig. 18 History match of oil production in well 4-12

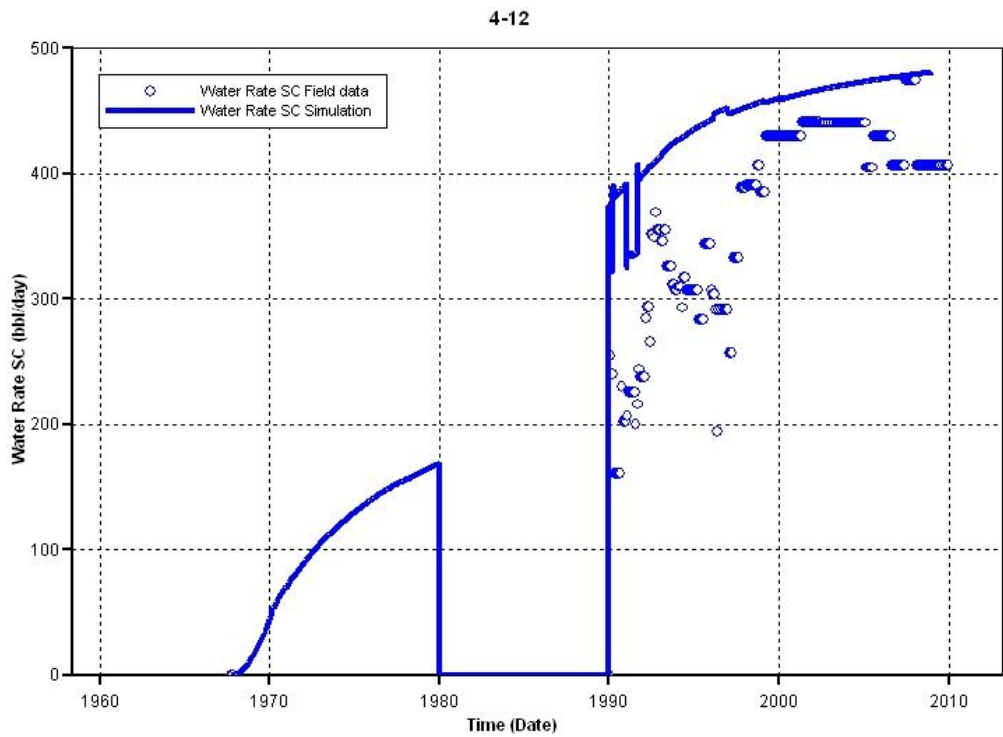


Figure 19 History match of water production in well 4-12

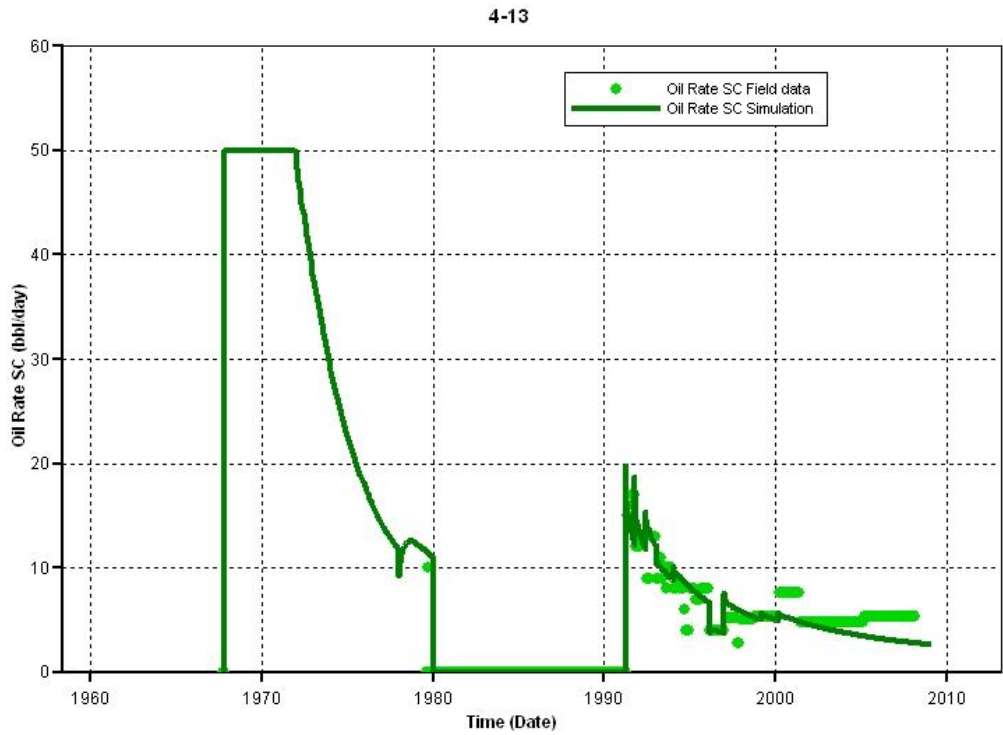


Figure 20 History match of oil production in well 4-13

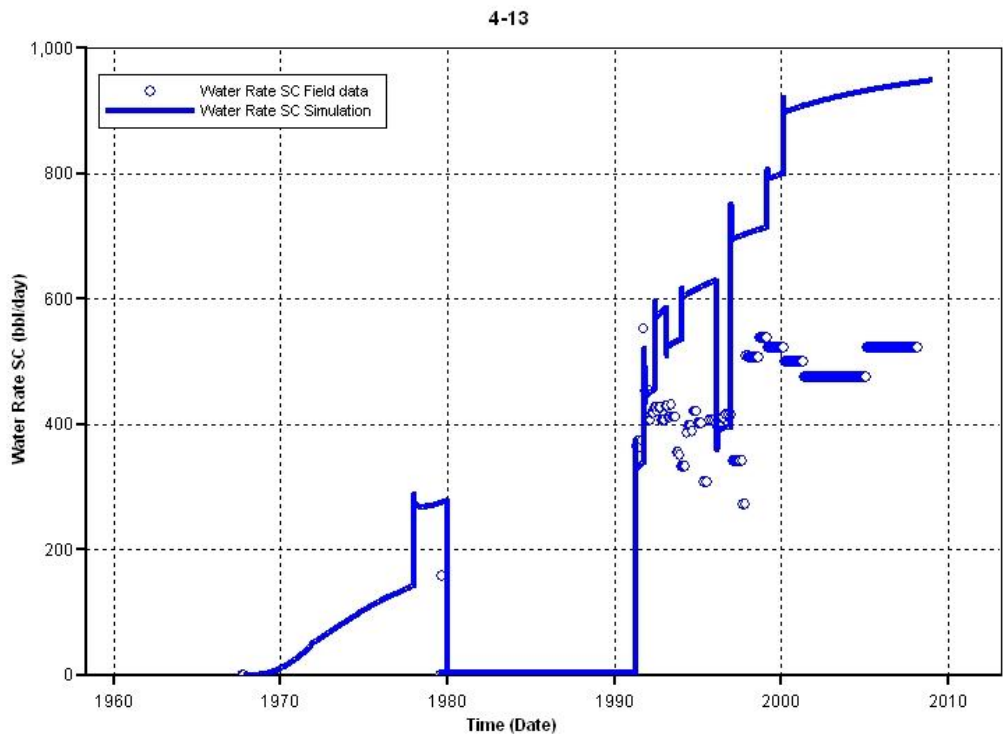


Figure 21 History match of water production in well 4-13

Although the Ogallah unit has been in production since 1951, the average reservoir pressure was not changed significantly. Figure 22 shows the average reservoir pressure based on the model calculation which decreases from 1200 psi to 1180 psi in 50 years of production. This confirms the assertion that the reservoir is underlain by an aquifer and the Carter-Tracery method is adequate to simulate the pressure support needed by the reservoir performance. As shown in the same figure, the average reservoir pressure in Lease 3, E. A. Scott varies between 1200 psi and 1150 psi.

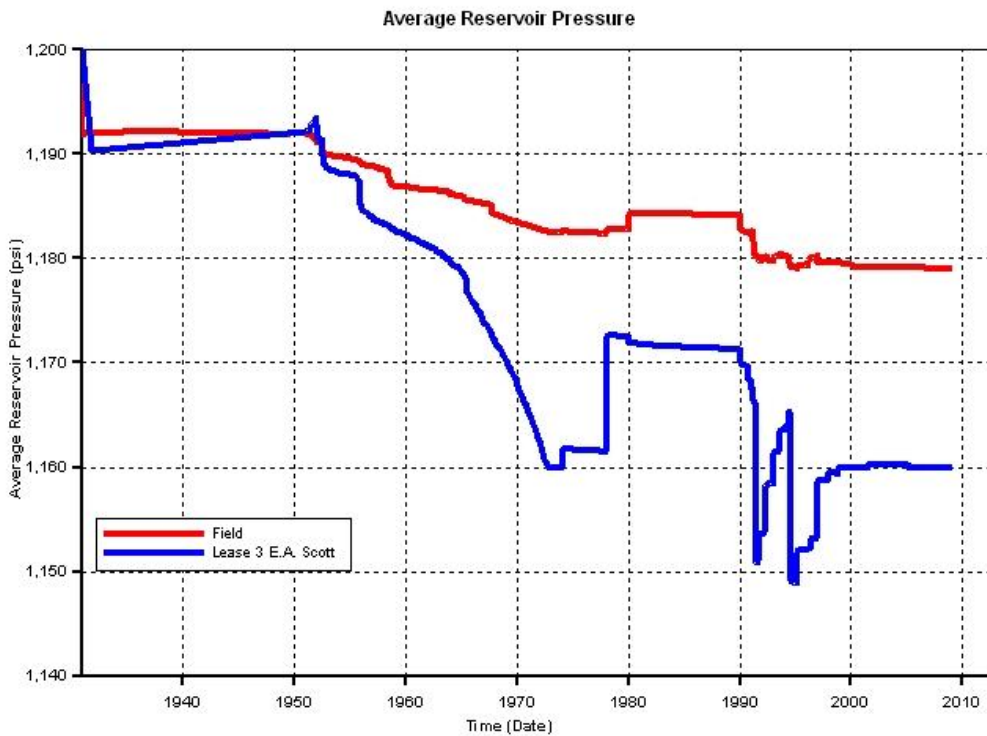


Figure 22 Average reservoir pressures of Ogallah unit and Lease E. A. Scott

Simulation of Carbon Dioxide Injection

The objective of CO₂ injection simulation is to investigate the feasibility of using CO₂ to improve oil recovery at near miscible condition in Ogallah unit. The reservoir model constructed in IMEX for history match was converted to GEM, a compositional simulator to simulate phase behavior of reservoir fluids for CO₂ injection process. All the reservoir properties after adjustment for the history match were kept intact in the compositional simulator. Compositional model was applied with the system consisting of oil in four components, water and carbon dioxide.

In the process of history match, verification of the modeling results was limited to a few wells having detailed production record. As a result, simulation of CO₂ injection is continued on selected wells with a reasonably well matched history. The Lease 3 was selected for further case study as it contains two wells with reasonably well matched production history in the model. The Lease 3 as seen in Figure 9 is located in central- west part of the field. It is surrounded by lease 1, 2, 4 and 13. Figure 23 shows the grid system of the lease presented in the reservoir model. The lease has four producers, well 3-1, 3-2, 3-3, and 3-4. Two producers (3-2 and 3-3) produces from Arbuckle, the other two (3-1 and 3-4) produces from Arbuckle and LKC. The size of the lease is approximately 47 acre. The pore volume calculated by the model was 3.64 MM bbl. At year 1951, the average oil saturation in the lease was 0.472 and the OOIP was 1.72 MM bbl. The properties of well blocks at these wells are summarized in Table 5. The properties at well 3-2 and 3-3 were adjusted for history match during the primary production whereas the properties at well 3-1 and 3-4 were maintained the same as that in the geological model. The scenarios designed for CO₂ injection are described as follows.

Table 5 Well block properties at well locations

Description	Well 3-2		Well 3-3	Well 3-1	Well 3-4
	Arbuckle	Reagan	Arbuckle	Arbuckle	Arbuckle
ϕ	0.164	0.201	0.203	0.123	0.119
k (md)	52.94	252.01	258.46	5.25	4.22
S _w	0.382	0.417	0.413	0.486	0.593

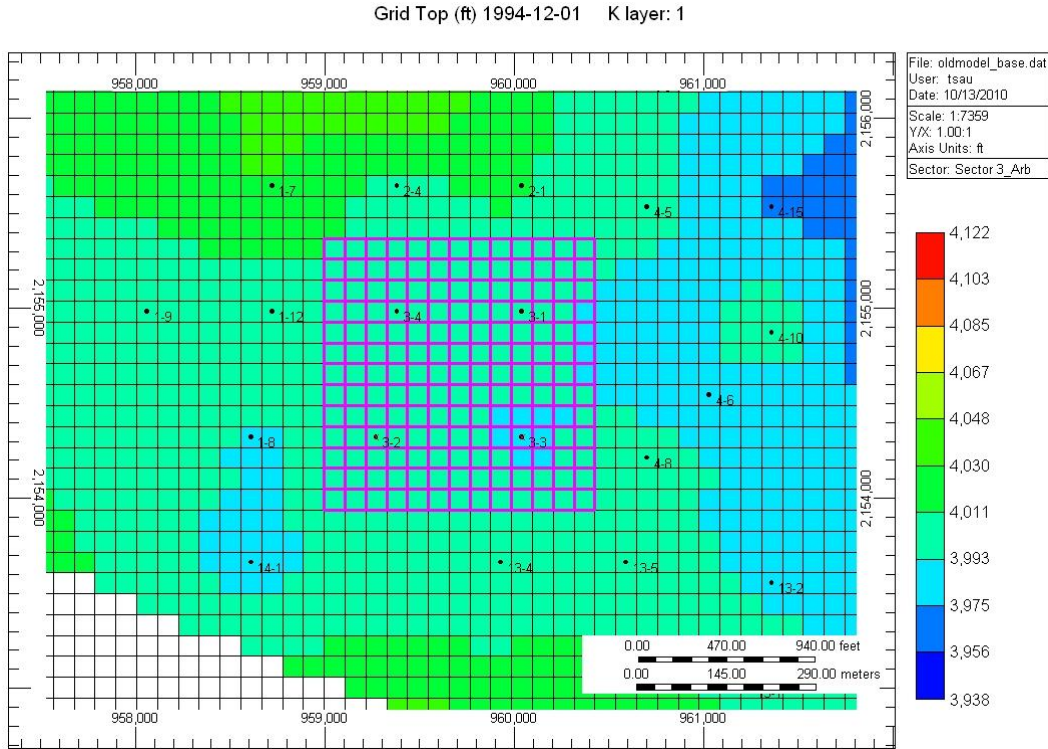


Figure 23 Grid system of Lease 3, E. A. Scott

One CO₂ Injector

The current status of well 3-1 is shut-in in the field while all other three remains open. Well 3-2 and 3-3 are producing from Arbuckle group whereas well 3-4 is in comingle production from Arbuckle and LKC. Therefore, only well 3-2 and 3-3 were considered to be converted to injector in the case study of one CO₂ injector.

Four cases were designed to simulate CO₂ injection process with one injector. In case 1, well 3-2 was converted to injector. CO₂ was injected at a maximum bottomhole pressure (BHP) of 1300 psi and a maximum rate of 200 MSCF/day. In case 2, well 3-2 injected CO₂ at BHP of 1200 psi and rate of 200 MSCF/day. In case 3, well 3-3 was converted to injector and injected CO₂ at BHP of 1300 psi with rate of 200 MSCF/day. In case 4, well 3-3 injected CO₂ at 1200 psi with a rate of 200 MSCF/day. In all cases, the CO₂ was injected on February 1, 2009 and continued for 10 years until February 1, 2019. When one injector injected CO₂, the remaining producers were open to production except well 3-1 was shut in. As a base case, the lease production was modeled without CO₂ injection until February 1, 2019

Figure 24 shows the production performance of well 3-2 when CO₂ was injected into well 3-3. The incremental oil is produced prior to the breakthrough of CO₂ when CO₂ is injected at 1300 psi. The water production of the same well is reduced (see Figure 25) as a result of CO₂ injection. Similar results are observed in well 3-3 when CO₂ is injected into well 3-2 (Figure 26 and 27). The comparisons of the results between two injection pressures with the base case are summarized in Table 6 and 7. The incremental oil in the base case is primarily produced by the natural water drive whereas in the other cases, it is attributed to CO₂ injection. It is apparent that the oil production is increased and water production is reduced when CO₂ is injected at pressure below MMP, 1350 psi. Since the average pressure of lease 3 at the start of CO₂ injection was 1160 psi in the model (as shown in Figure 22), less CO₂ is injected at a lower pressure. Nevertheless, fair amount of incremental oil is recovered as a result of CO₂ injection which shows the benefits of using CO₂ as a displacing agent to recover oil at near miscible condition. The gross utilization of CO₂ in all of the cases varies from 17 to 33 MCF/STB whereas net utilization of CO₂ varies from 12 to 27 MCF/STB. The CO₂ retention efficiency, which is the amount of CO₂ remained in the reservoir after 10 years of injection and production, varies from 59 to 83%.

Table 6 Comparison of incremental oil and water production in 10 years of CO₂ injection

CO ₂ injected at well 3-3 and produced at well 3-2					
	CO ₂ Injected	CO ₂ Produced	CO ₂ Remained	Oil	Water
	(SCF)	(SCF)	(SCF) (%)	(STB)	(STB)
Base case				11237	2319200
Case 1 @1300 psi	7.25E+08	3.01E+08	4.24E+08 (59)	34205	1984420
Case 2 @1200 psi	4.88E+08	1.55E+08	3.33E+08 (68)	28412	2106800

Table 7 Comparison of incremental oil and water production in 10 years of CO₂ injection

CO ₂ injected at well 3-2 and produced at well 3-3					
	CO ₂ Injected	CO ₂ Produced	CO ₂ Remained	Oil	Water
	(SCF)	(SCF)	(SCF) (%)	(STB)	(STB)
Base case				7266	684100
Case 1 @1300 psi	7.30E+08	1.44E+08	5.86E+08 (80)	21895	431070
Case 2 @1200 psi	6.53E+08	1.12E+08	5.41E+08 (83)	19809	464930

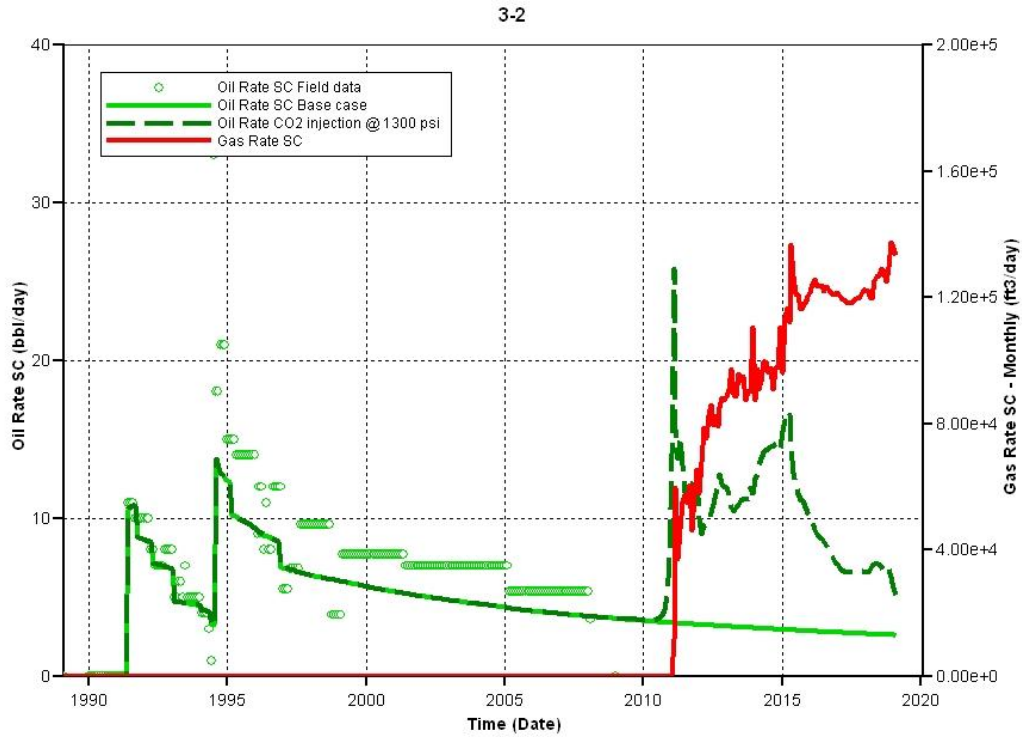


Figure 24 Incremental oil productions at well 3-2 when CO₂ was injected at well 3-3

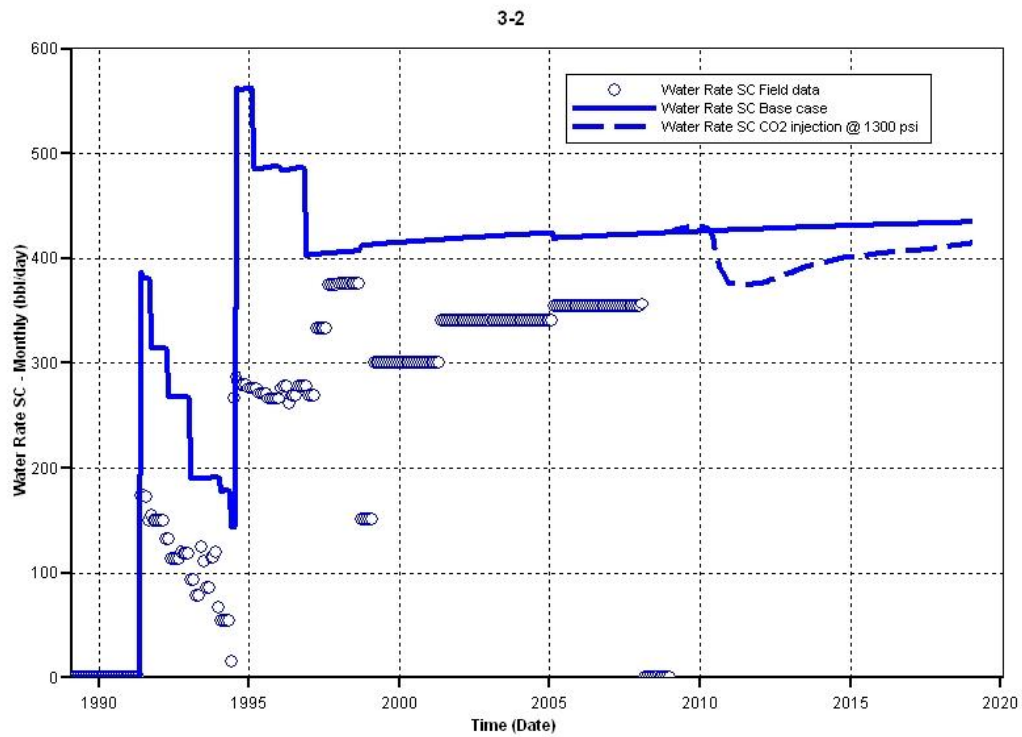


Figure 25 Reduction of water production at well 3-2 when CO₂ was injected at well 3-3

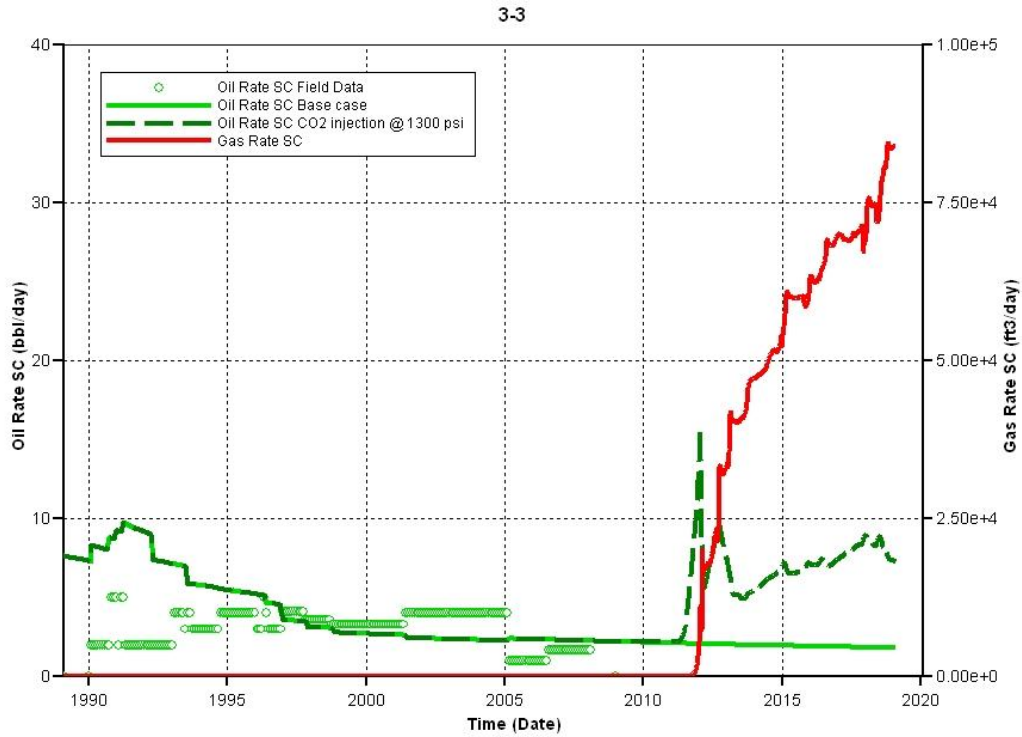


Figure 26 Incremental oil productions at well 3-3 when CO₂ was injected at well 3-2

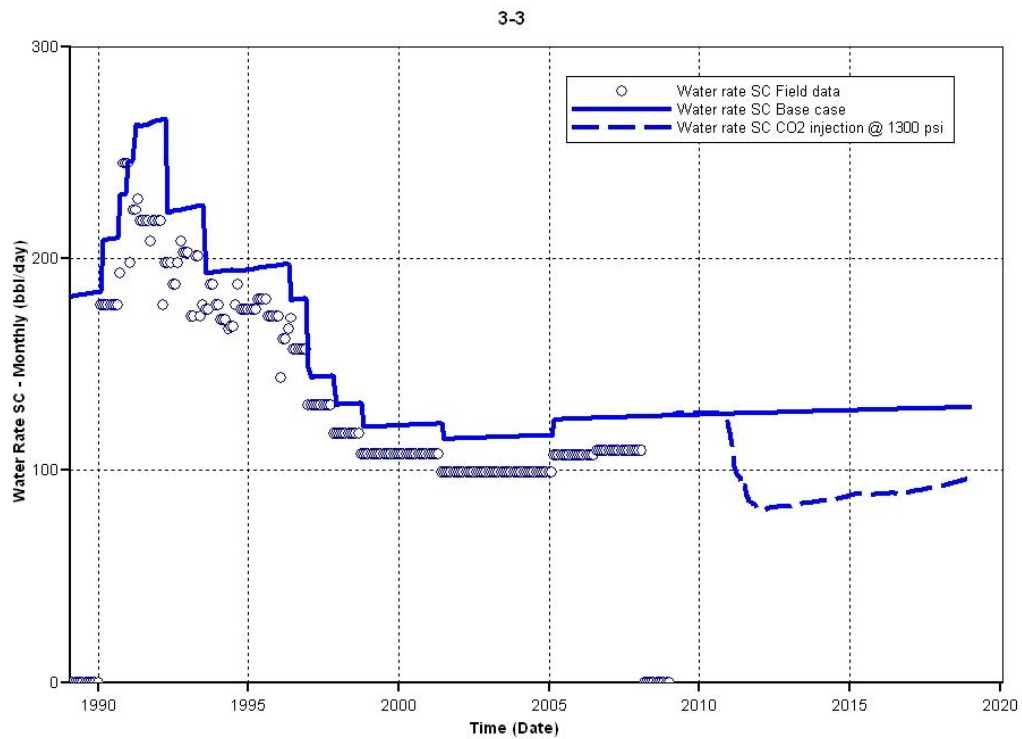


Figure 27 Reduction of water production at well 3-3 when CO₂ was injected at well 3-2

Two CO₂ Injectors

To extend the modeling of CO₂ injection at Lease 3 with two injectors, case study was designed to study the effect of injection pattern on oil recovery and CO₂ sequestration in the reservoir. The pattern design is shown in Figure 28 where the ratio of injector to producer is one to one. The lease itself is surrounded by lease 1, 2, 4 and 13. Field production data indicate that well 3-2 and well 3-3 are two of the better producers in the lease. When either one is converted to a CO₂ injector, 200 MSCF/day of CO₂ can be injected without exceeding the formation fracture pressure. In each of the injection pattern, the maximum injection rate of each injector was set at 200 MSCF/day. The bottomhole pressure was set at either 1200 or 1300 psi. The simulated injection rate, however, varied from case to case depending on the injectivity of the well and the flow pattern of the CO₂ which is affected by the reservoir heterogeneity.

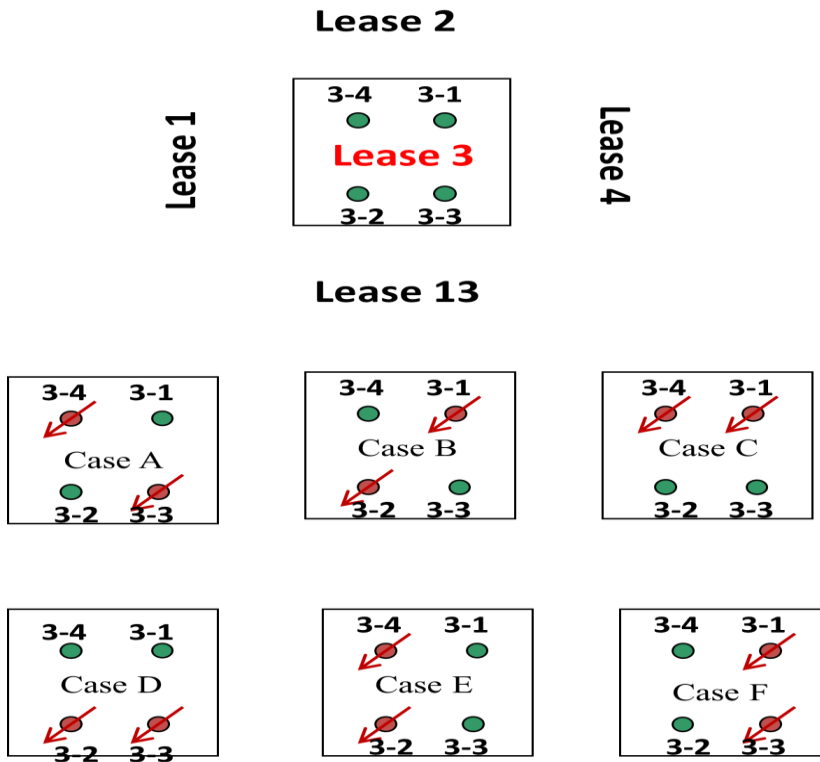


Figure 28 Pattern design of lease 3 for CO₂ injection

The primary production without CO₂ injection was simulated with all four producers open for production. The production performance from February 1, 2009 to February 1, 2019 was referred as a base case in which the recovery mechanism is relied on the natural water drive

from the underlying aquifer. The recovery efficiency from the primary production in this 10 year span was compared with the results from CO₂ IOR at near miscible condition.

Generally, the incremental oil recovery is increased with the injection pressure as more CO₂ is injected and interacted with oil during the displacement process. The recovery results differ in each case which is attributed to the variation in remaining oil in place at the beginning of CO₂ injection and the flow path of the displacing agent. Because there is no water injector around the lease to confine CO₂, CO₂ concentration remained in the lease at the end of injection depends on the flow direction and capacity of CO₂. Figure 29 to Figure 34 present remaining CO₂ concentrations in the lease 3 and its surrounding leases at the end of injection. It shows that CO₂ tends to move towards lease 13 and lease 1 which is located at west and south part of lease 3. As a result, the incremental oil produced from these surrounding leases is attributed to the CO₂ injection. When the injection pressure is limited at 1300 psi, the highest incremental oil recovery occurs in case A where CO₂ was injected in wells 3-4 and 3-3. The recovery factor increases from 32.7 to 36.3% (Figure 35). At a lower injection pressure, 1200 psi, the recovery factor is reduced to 34%. If the maximum injection rate, 200 MCF/day is maintained for each injector in the designed pattern, the recovery efficiency becomes 37.5%, an increase of 4.8%.

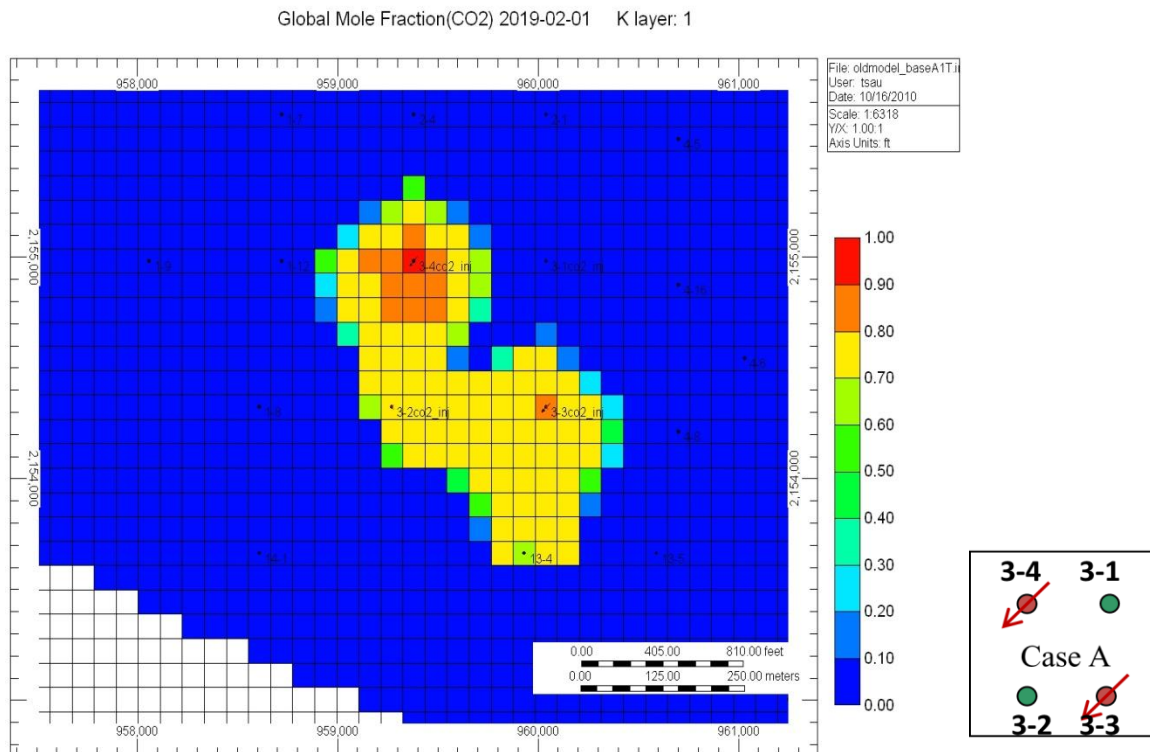


Figure 29 CO₂ distributions after 10 years of injection, Case A1

Global Mole Fraction(CO2) 2019-02-01 K layer: 1

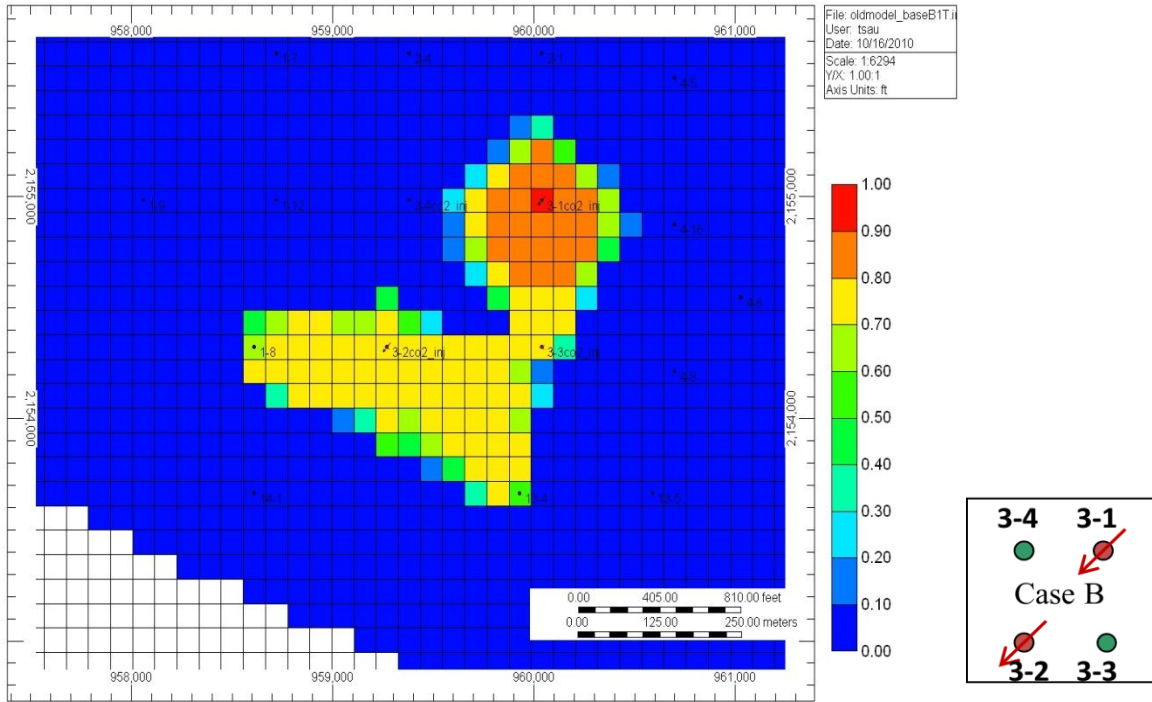


Figure 30 CO₂ distributions after 10 years of injection, Case B1.

Global Mole Fraction(CO2) 2019-02-01 K layer: 1

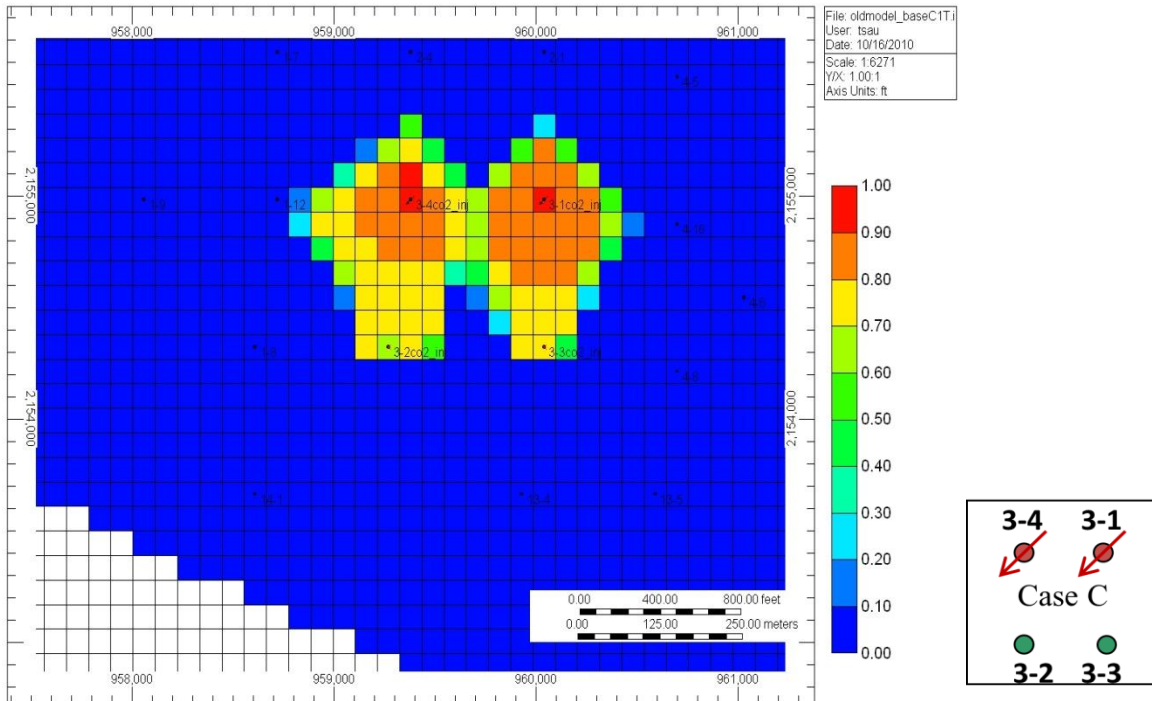


Figure 31 CO₂ distributions after 10 years of injection, Case C1.

Oil Mole Fraction(CO2) 2019-02-01 K layer: 1

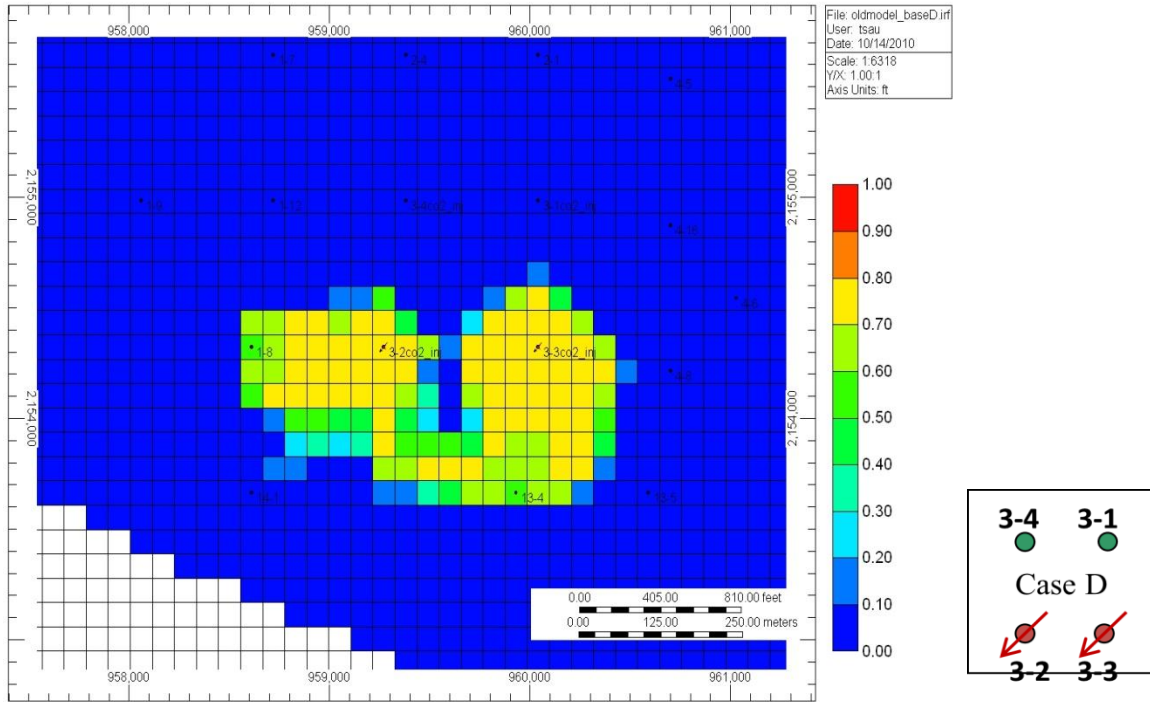


Figure 32 CO₂ distributions after 10 years of injection, Case D1.

Global Mole Fraction(CO2) 2019-02-01 K layer: 1

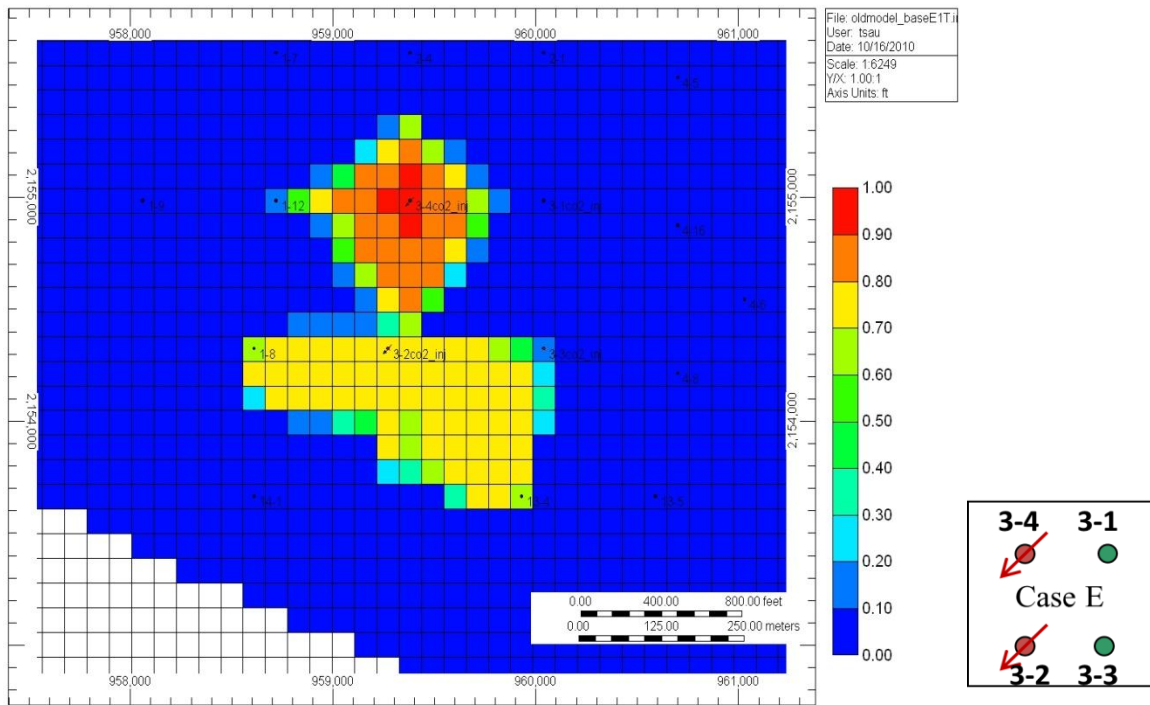


Figure 33 CO₂ distributions after 10 years of injection, Case E1.

Global Mole Fraction(CO2) 2019-02-01 K layer: 1

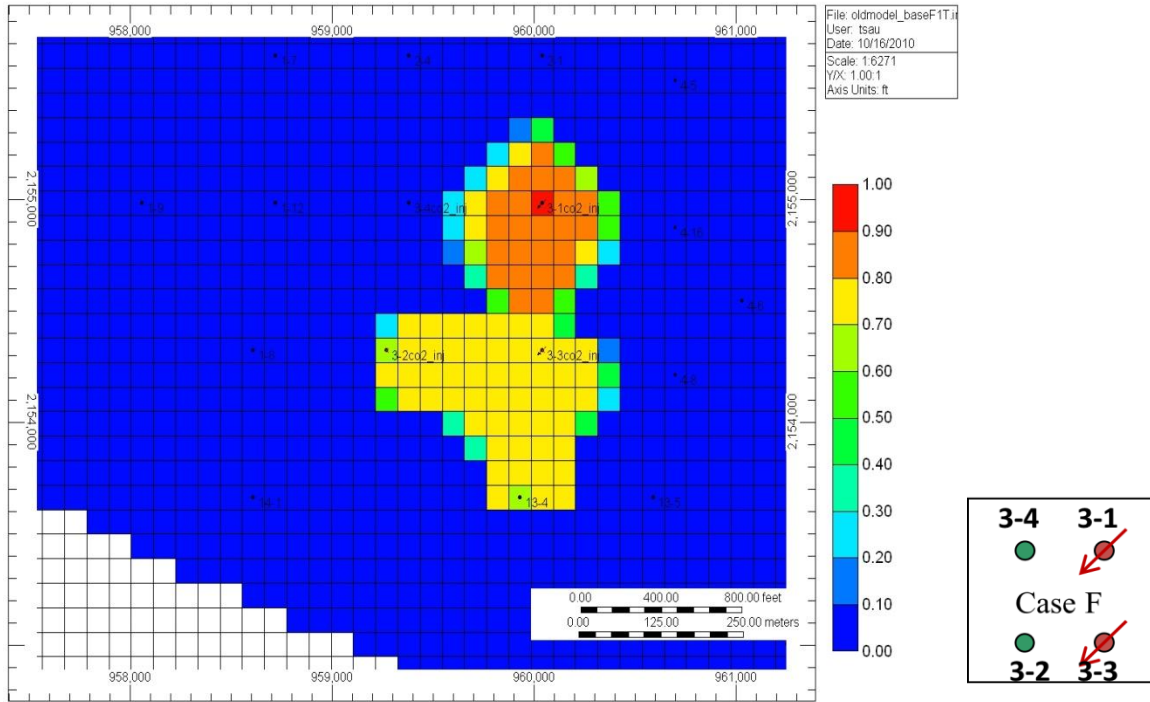


Figure 34 CO₂ distributions after 10 years of injection, Case F1.

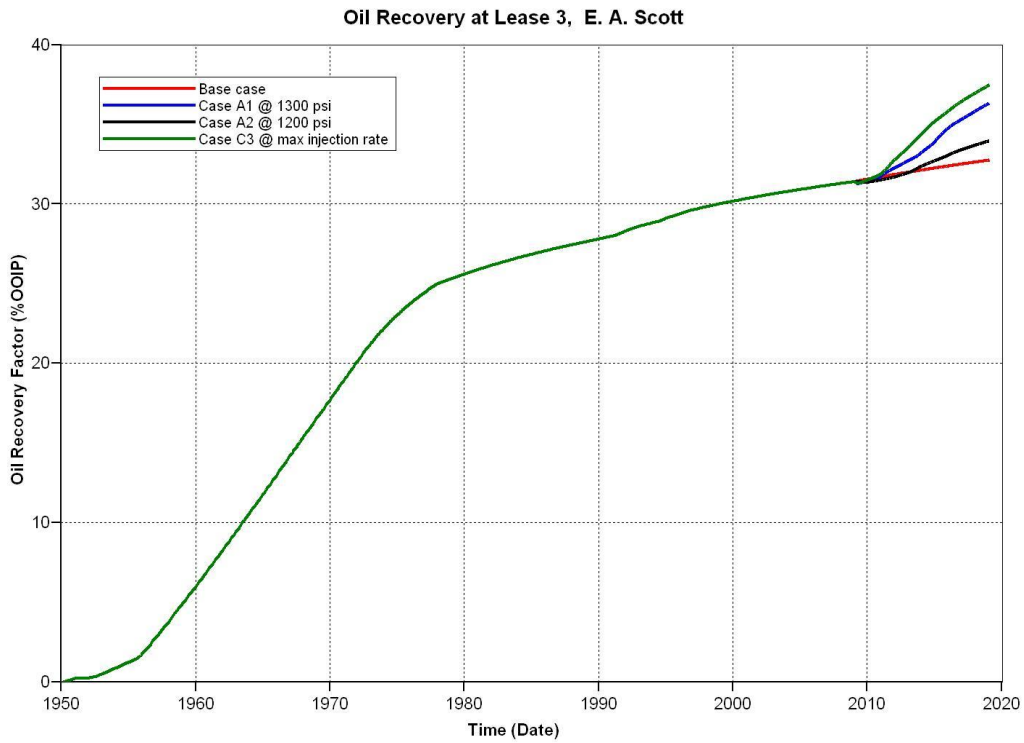


Figure 35 Comparison of oil recovery factors at Lease 3

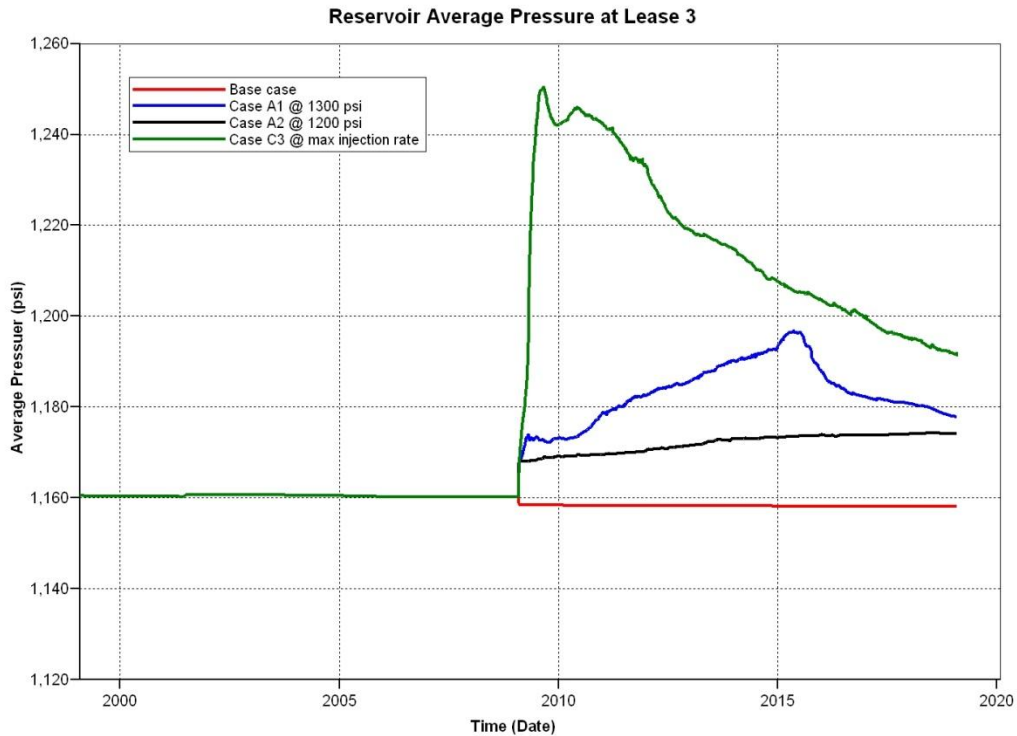


Figure 36 Average reservoir pressures at Lease 3 with/without CO₂ injection

The average reservoir pressure in the lease in all cases is below 1300 psi and above 1150 psi. Figure 36 shows the pressure history during CO₂ injection. When the BHP of injector is controlled at 1300 psi for well 3-3 and 3-4, the average reservoir slightly increases and never reaches the initial reservoir pressure of 1200 psi. When the maximum injection rate, 200 MSCF/day is maintained during the injection such as in Case C3, the average reservoir pressure rises above the initial reservoir pressure at the early stage of injection and declines to below that at the late stage of injection. When the BHP of injector is controlled at 1200 psi such as in the Case A2, the reservoir pressure only increases slightly. In all the cases, nevertheless, the reservoir pressure is within the near miscible condition in which the recovery efficiency benefits from the improvement of relative mobility ratio of the CO₂ and oil and the efficacy of CO₂ extraction as demonstrated in the laboratory core flood study. However, the recovery efficiency is significantly affected by the reservoir heterogeneity which results in less improvement of oil production within the lease.

Detailed modeling results are summarized in Table 8 to Table 10. The CO₂ injected, produced and remained in the lease are listed in each table. The total incremental oil production resulting from the CO₂ injection is compared with the base case. The utilization of CO₂ and CO₂

retention percentage in each case are also calculated. The area sweep efficiency is affected by the reservoir heterogeneity. CO₂ injectors placed in well 3-4 and well 3-3 as in pattern case A performed better than the other patterns. A higher injection pressure of CO₂ also results in a better recovery performance. Depending on the injection pattern, the net utilization of CO₂ can be as low as 2 MSCF/STB and as high as 20 MSCF/STB. The effective CO₂ storage percentage in lease 3 can be as low as 3% and as high as 63% based on the theoretical storage capacity of 1.58 BSCF.

The theoretical CO₂ sequestration capacity is calculated based on the rock volume, porosity, initial oil saturation, and recovery factor. For reservoir underlain by an aquifer, the reservoir CO₂ sequestration capacity is reduced by the water influx from the aquifer but is augmented by the volume of water produced. The capacity for CO₂ sequestration in this case is given by equation (6)

$$V_{CO_2} = (A \times h) \times \phi \times RF \times S_{oi} - V_{flux} + V_{wp} \quad (6)$$

where V_{CO_2} : reservoir volume of CO₂ sequestered

A : area

h : thickness of formation

ϕ : porosity

RF : recovery factor

S_{oi} : initial oil saturation

V_{flux} : cumulative water influx

V_{wp} : cumulative water produced

Based on the reservoir model calculation, the pore volume of lease 3 is 3.64 MM bbl, average initial oil saturation is 0.472. The recovery factor of the primary production from 1951 to 2019 is 0.327 as shown in Figure 37. The cumulative water influx is 10.5 MM bbl and cumulative water production is 11.9 MM bbl. The capacity of CO₂ sequestration is 1.86 MM bbl which is 10.4 MMCF at reservoir condition (1200 psig and 110 °F) or 1.58 BSCF at standard condition.

Table 8 Result of case study with CO₂ injection at BHP of 1300 psi

	Base case	Case A1	Case B1	Case C1	Case D1	Case E1	Case F1
CO ₂ Injected (SCF)		1.23E9	9.89E8	7.58E8	1.45E9	1.15E9	9.36E8
CO ₂ Produced (SCF)		6.98E8	3.04E8	2.70E8	7.17E8	3.12E8	4.96E8
CO ₂ Remained (SCF)		5.34E8	6.84E8	4.88E8	7.29E8	8.35E8	4.40E8
Incremental oil from lease 3 (STB)	25473	60828	31443	54345	7292	26737	35394
Incremental oil from lease 13 (STB)	0	7620	11470	0	21700	12680	7380
Incremental oil from lease 4 (STB)	0	0	233	228	158	7	324
Incremental oil from lease 1 (STB)	0	153	9078	314	11533	10305	10
Incremental oil from lease 2 (STB)	0	7	9	19	0	11	9
Incremental oil Total (STB)	25473	68608	52233	54915	40683	49740	43117
Incremental oil relative to Base case		43135	26760	29442	15210	24267	17644
Water production (STB)	1.19E7	1.05E7	9.24E6	1.13E7	9.17E6	9.20E6	1.08E7
GU (MCF/STB)		18	19	14	36	23	22
NU (MCF/STB)		8	13	9	18	17	10
CO ₂ retention %		43	69	64	50	73	47
Effective storage %		34	43	31	46	53	28

Table 9 Result of case study with CO₂ injection at BHP of 1200 psi

	Base case	Case A2	Case B2	Case C2	Case D2	Case E2	Case F2
CO ₂ Injected (SCF)		5.20E8	6.60E8	4.09E7	7.23E8	6.50E8	4.92E8
CO ₂ Produced (SCF)		2.57E8	2.14E8	0	2.01E8	2.19E8	2.61E8
CO ₂ Remained (SCF)		2.64E8	4.46E8	4.09E7	5.22E8	4.31E8	2.31E8
Incremental oil from lease 3 (STB)	25473	34207	21251	18623	7177	24871	29811
Incremental oil from lease 13 (STB)	0	6200	7650	0	9740	8320	6190
Incremental oil from lease 4 (STB)	0	0	9	4	42	0	50
Incremental oil from lease 1 (STB)	0	0	7904	6	8575	7955	5
Incremental oil from lease 2 (STB)	0	0	0	0	0	1	1
Incremental oil Total (STB)	25473	40407	36814	18633	25534	41147	36057
Incremental oil relative to Base case		14934	11341	(6840)	61	15674	10584
Water production (STB)	1.19E7	1.05E7	9.28E6	1.07E7	8.90E6	9.23E6	1.09E7
GU (MCF/STB)		13	18	2	28	16	14
NU (MCF/STB)		7	12	2	20	10	6
CO ₂ retention %		51	68	100	72	66	47
Effective storage %		17	28	3	33	27	15

Table 10 Result of case study with CO₂ injection at 200 MSCF/day/well

	Base case	Case A3	Case B3	Case C3	Case D3	Case E3	Case F3
CO ₂ Injected (SCF)		1.45E9	1.45E9	1.45E9	1.45E9	1.45E9	1.45E9
CO ₂ Produced (SCF)		8.18E8	6.07E8	7.42E8	7.17E8	4.39E8	7.02E8
CO ₂ Remained (SCF)		6.27E8	8.38E8	7.03E8	7.29E8	1.01E9	7.44E8
Incremental oil from lease 3 (STB)	25473	65375	48399	75206	7292	29452	58510
Incremental oil from lease 13 (STB)	0	7830	12670	0	21700	14680	10580
Incremental oil from lease 4 (STB)	0	0	1051	1085	158	7	1450
Incremental oil from lease 1 (STB)	0	3374	10038	3920	11533	16766	11
Incremental oil from lease 2 (STB)	0	0	59	97	0	35	73
Incremental oil Total (STB)	25473	76579	72217	80308	40683	60940	70642
Incremental oil relative to Base case		51106	46744	54835	15210	35467	45151
Water production (STB)	1.19E7	1.05E7	9.15E6	1.07E7	8.90E6	9.20E6	1.07E7
GU (MSCF/STB)		19	20	18	36	24	20
NU (MSCF/STB)		8	12	9	18	17	11
CO ₂ retention %		43	58	49	50	70	51
Effective storage %		39	53	44	46	63	47

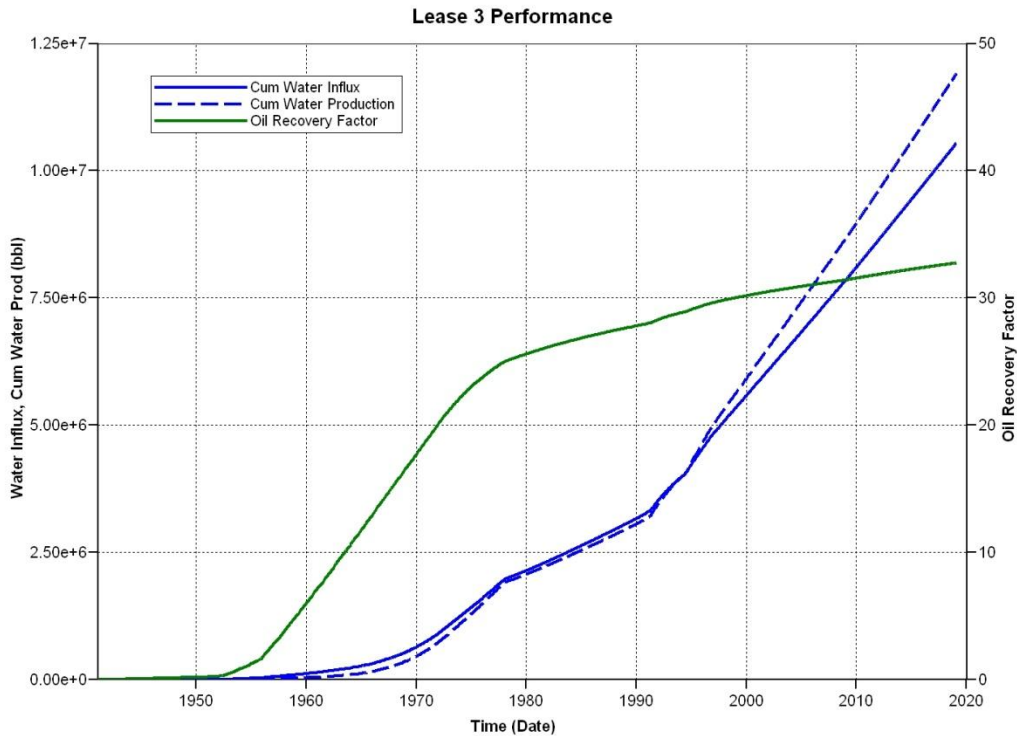


Figure 37 Lease 3 production performance without CO₂ injection

For the field application, the theoretical CO₂ storage capacity can be estimated with given information in equation (6) from the reservoir model or reserve database and production history. Precise estimates of the effective CO₂ sequestration capacity during CO₂ IOR operations, however, requires numerical reservoir simulation because of the nature of the displacement process and the reservoir heterogeneity,

The results presented in this section demonstrate the effect of pattern design and injection pressure and rate on the oil recovery efficiency and CO₂ sequestration. In general, it shows that improvement of oil recovery at near miscible condition is achievable under current reservoir operation pressure. The oil recovery efficiency and CO₂ sequestration capacity vary with the injection pattern which can be further investigated when the target area is extended to a whole field study.

Because uncertainties still exist in the current reservoir model where most of reservoir properties are not verified by the history match process, the estimation of oil recovery and CO₂ storage capacity for the whole field is not implemented until further verification is completed. Plan to verify current reservoir model is underway by reviewing fourteen cored well data obtained lately. These wells are located at lease 1, 6, 7, 10 and 11 which are in the west, central

east, and southeast part of the field. Including these cored data with well logging interpretation will enhance the understanding and certainty about the current geological model and improve the model in prediction of reservoir performance. In addition, an evaluation plan devised to better understand this reservoir is proposed and will proceed in the near future. The proposed plan is to conduct tests to seek data that pertain to the pressure, residual oil saturation, reservoir properties and the nature of the flow from well to well in the reservoir. The tests will include single well transient pressure tests, multiple well interference tests, single well tracer tests and interwell tracer tests. With the current reviewing plan and future proposed tests, the current reservoir model is to be calibrated with a better reservoir description. The effect of reservoir heterogeneity on process performance will be reevaluated. The updated reservoir simulation results will be delivered when it is available.

4. Summary

1. The geological model was developed based on well-log interpretation and cross-plotting method. An in-house developed correlation between resistivity log and porosity log was successfully applied to calculate porosity based on microlog measurements.
2. The primary production history of a 47 acre lease (lease 3) containing four wells was reasonably matched. This lease was extensively examined for near miscible CO₂ injection process.
3. The simulation results indicate that near miscible displacement is achievable in lease 3 at current reservoir operation pressure. The incremental oil recovery generally increases with the injection pressure. The oil recovery efficiency was increased by 1.3 to 4.8% as a result of CO₂ injection.
4. The oil recovery efficiency and CO₂ sequestration capacity depend on the implementation of CO₂ injection which includes injection pressure, rate and pattern design.
5. The theoretical storage capacity of CO₂ in lease 3 was 1.58 BSCF. The net utilization of CO₂ in IOR process varied from 8 to 18 MSCF/STB when 1.45 BSCF CO₂ was injected in 10 years. The effective storage capacity of CO₂ varied from 39 to 63% at the end of CO₂ injection.

References

Byrnes, A. P., Franseen, E. K. and Steinhaff, D. M.: "Integrating plug to well-scale petrophysics with detailed sedimentology to quantify fracture, vug and matrix properties in carbonate reservoirs; an example from the Arbuckle Group, Kansas." University of Kansas, (pp.3) 1999.

Bui, L.H., Tsau, J.S., and Willhite, G. P.: "Laboratory Investigations of CO₂ Near Miscible Application in Arbuckle Reservoir" paper SPE-129710 to be presented at 2010 SPE Improved Oil Recovery Symposium, Tulsa, April 24-28.

Corey, A. T., "The Interrelations Between Gas and Oil Relative Permeabilities," Producers Monthly (Nov 1954), Vol. 19, p 38-41.

Franseen, E. K., Byrnes, A. P., Cansel, J.R., Steinhaff, D. M., and Carr, T. R.: "The Geology of Kansas ARBUCKLE GROUP", *Current Research in Earth Sciences*, Bulletin 250, part 2.

Franseen, E. K., Byrnes, A. P., Cansel, J.R., Steinhaff, D. M., and Carr, T. R., and Dubois, M.K.: "Geologic Controls on Variable Character of Arbuckle Reservoirs in Kansas-An Emerging Picture," Kansas Geological Survey, Open-file Report 2003-59

Tsau, J. S.: "Near Miscible CO₂ Application to Improve Oil Recovery for Small Producers," RPSEA Technical Report 07123-03.01, 2010.